

文書²¹⁾を公表している。また、研究開発が進むiPS細胞等の多能性幹細胞に由来するATMPに関する特別な留意点をまとめた文書²²⁾を公表するなど、EUの医薬品産業の強化に必要な新技術の開発支援に積極的な姿勢を示している。

細胞・組織加工製品を医薬品か医療機器かに分類するのではなく、ATMPという医薬品カテゴリーに括って特別な規制をかける、というEUの非常に大胆な取り組みは、従来の医薬品・医療機器の二分法に拘泥されずに先端医療製品そのものと率直に向き合いつつ品質・安全性・有効性の評価を行うことができる可能性を持っている。あらゆる医療製品や医療技術が究極的には患者あるいは将来、患者になりうる人々のために制度上も最も効果的、合理的なアプローチをとるという視点で考えれば、むしろ必然的な帰結であるかも知れない。我が国における先端医療の実用化促進施策、及び規制の国際協調のためにも参考とすべきものと考えられる。

文 献

- 1) Directive 2001/83/EC of the European Parliament and of the Council of 6 November 2001 on the Community code relating to medicinal products for human use.
- 2) Commission Directive 2003/63/EC of 25 June 2003 amending Directive 2001/83/EC of the European Parliament and of the Council on the Community code relating to medicinal products for human use.
- 3) Council Directive 93/42/EEC of 14 June 1993 concerning medical devices.
- 4) Council Directive 90/385/EEC of 20 June 1990 on the approximation of the laws of the Member States relating to active implantable medical devices.
- 5) Regulation (EC) No 1394/2007 of the European Parliament and of the Council of 13 November 2007 on advanced therapy medicinal products and amending Directive 2001/83/EC and Regulation (EC) No 726/2004.
- 6) Commission Directive 2009/120/EC of 14 September 2009 amending Directive 2001/83/EC of the European Parliament and of the Council on the Community code relating to medicinal products for human use as regards advanced therapy medicinal products.
- 7) EMA: Guideline on human cell-based medicinal products EMEA/CHMP/410869/2006.
- 8) EMA: Concept paper on the development of a guideline on the risk-based approach according to annex I, part IV of directive 2001/83/EC applied to advanced therapy medicinal products EMA/CHMP/CPWP/708420/2009.
- 9) Directive 2004/23/EC of the European Parliament and of the Council of 31 March 2004 on setting standards of quality and safety for the donation, procurement, testing, processing, preservation, storage and distribution of human tissues and cells.
- 10) Commission Directive 2006/17/EC of 8 February 2006 implementing Directive 2004/23/EC of the European Parliament and of the Council as regards certain technical requirements for the donation, procurement and testing of human tissues and cells.
- 11) Commission Directive 2006/86/EC of 24 October 2006 implementing Directive 2004/23/EC of the European Parliament and of the Council as regards traceability requirements, notification of serious adverse reactions and events and certain technical requirements for the coding, processing, preservation, storage and distribution of human tissues and cells.
- 12) Commission Directive 2003/94/EC of 8 October 2003 laying down the principles and guidelines of good manufacturing practice in respect of medicinal products for human use and investigational medicinal products for human use.
- 13) EMA: GMP for advanced therapy medicinal products: status EMEA/INS/GMP/372447/2008.
- 14) EMA: Guideline on safety and efficacy follow-up-risk management of advanced therapy medicinal products EMEA/149995/2008.
- 15) Directive 2002/98/EC of the European Parliament and of the Council of 27 January 2003 setting standards of quality and safety for the collection, testing, processing, storage and distribution of human blood and blood components and amending Directive 2001/83/EC.
- 16) Directive 95/46/EC of the European Parliament and of the Council of 24 October 1995 on the protection of individuals with regard to the processing of personal data and on the free movement of such data.
- 17) Directive 2001/20/EC of the European Parliament and of the Council of 4 April 2001 on the approximation of the laws, regulations and administrative provisions of the Member States relating to the implementation of good clinical practice in the conduct of clinical trials on medicinal products for human use.
- 18) European Commission: Detailed guidelines on good clinical practice specific to advanced therapy medicinal products ENTR/F/2/SF/dn D (2009) 35810 (3 December 2009).
- 19) Heads of Medicines Agencies: Guidance document for a Voluntary Harmonisation Procedure (VHP) for the assessment of multinational Clinical Trial Applications CTFG//VHP/2010/Rev1.
- 20) European Commission: Consultation paper: Human tissue engineering and beyond: proposal for a community regulatory framework on advanced therapies (4 May 2005).
- 21) EMA: Reflection paper on in-vitro cultured chondrocyte containing products for cartilage repair of the knee CAT/CPWP/568181/2009.
- 22) EMA: Reflection paper on stem cell-based medicinal products (draft) CAT/571134/09.

Glycosylation Analysis of IgLON Family Proteins in Rat Brain by Liquid Chromatography and Multiple-Stage Mass Spectrometry[†]

Satsuki Itoh,[‡] Akiko Hachisuka,[‡] Nana Kawasaki,^{*,‡,§} Noritaka Hashii,[‡] Reiko Teshima,[‡] Takao Hayakawa,^{||} Toru Kawanishi,[‡] and Teruhide Yamaguchi[‡]

Division of Biological Chemistry and Biologicals, National Institute of Health Sciences, 1-18-1, Kamiyoga, Setagaya-ku, Tokyo 158-8501, Japan, Core Research for Evolutional Science and Technology of Japan Science and Technology Agency, Kawaguchi Center Building, 4-1-8 Hon-cho, Kawaguchi, Saitama 332-0012, Japan, and Pharmaceutical Research and Technology Institute, Kinki University, 3-4-1 Kowakae, Higashi-Osaka 577-8502, Japan

Received May 23, 2008; Revised Manuscript Received July 17, 2008

ABSTRACT: IgLON family proteins, including limbic-associated membrane protein (LAMP), opioid-binding cell adhesion molecule (OBCAM), neurotrimin, and Kilon, are immunoglobulin (Ig) superfamily cell adhesion molecules. These molecules are composed of three Ig domains and a glycosylphosphatidylinositol (GPI) anchor and contain six or seven potential N-glycosylation sites. Although their glycosylations are supposed to be associated with the development of the central nervous system like other Ig superfamily proteins, they are still unknown because of difficulty in isolating individual proteins with a high degree of homology in performing carbohydrate analysis. In this study, we conducted simultaneous site-specific glycosylation analysis of rat brain IgLON proteins by liquid chromatography and multiple-stage mass spectrometry (LC–MSⁿ). The rat brain GPI-linked proteins were enriched and separated by sodium dodecyl sulfate–polyacrylamide gel electrophoresis. The four proteins were extracted from the gel, and subjected to LC–MSⁿ after proteinase digestions. A set of glycopeptide MS data, including the mass spectrum, the mass spectrum in the selected ion monitoring mode, and the product ion spectra, was selected from all data based on carbohydrate-related ions in the MS/MS spectrum. The peptide portion and the carbohydrate structure were identified on the basis of peptide-related ion and carbohydrate-related ions, and the accurate mass. The site-specific glycosylations of four proteins were elucidated as follows. *N*-Glycans near the N-terminal were disialic acid-conjugated complex- and hybrid-type oligosaccharides. The first Ig domains were occupied by Man-5-9. Diverse oligosaccharides, including Lewis *a/x*-modified glycans, a brain-specific glycan known as BA-2, and Man-5, were found to be attached to the third Ig domain. Three common structures of glycans were found in the GPI moiety of LAMP, OBCAM, and neurotrimin.

Cell adhesion molecules on cell surfaces are involved in several biological events, such as cell–cell interaction, signaling, and cellular traffic. In the central nervous system, cell adhesion molecules are associated with the differentiation and migration of neurons, and neurite outgrowth. The immunoglobulin (Ig) superfamily, which contains one or more Ig-like domains, is known as one of the cell adhesion molecule families in the central nervous system (1). The Ig superfamily includes various proteins, such as P0, Thy-1, myelin-associated glycoprotein (MAG), neural cell adhesion molecule (NCAM), L1, contactin, and IgLON family proteins. Glycosylation of the Ig superfamily proteins is known

to be involved in cell–cell interactions (2–4). Polysialylated glycans in the fifth domain of NCAM are thought to inhibit the interaction of NCAM with other molecules and to promote neural plasticity through a repulsive interaction (5, 6). The HNK-1 epitope in the third and fifth domains of NCAM is known to mediate molecular recognition in the nervous system (7).

The IgLON superfamily includes the limbic-associated membrane protein (LAMP),¹ the opioid-binding cell adhesion molecule (OBCAM), neurotrimin, and Kilon (8–14), and

[†] This work was supported in part by a Grant-in-Aid from the Ministry of Health and Labor and Welfare, and Core Research for Evolutional Science and Technology Program (CREST) of the Japan Science and Technology Agency (JST).

* To whom correspondence should be addressed: Division of Biological Chemistry and Biologicals, National Institute of Health Sciences, 1-18-1, Kamiyoga, Setagaya-ku, Tokyo 158-8501, Japan. Telephone: +81-3-3700-9074. Fax: +81-3-3707-6950. E-mail: nana@nihs.go.jp.

[‡] National Institute of Health Sciences.

[§] Core Research for Evolutional Science and Technology of Japan Science and Technology Agency.

^{||} Kinki University.

¹ Abbreviations: LC, liquid chromatography; MS, mass spectrometry; MSⁿ, multiple-stage mass spectrometry; LAMP, limbic-associated membrane protein; OBCAM, opioid-binding cell adhesion molecule; GlcNAc, *N*-acetylglucosamine; GPI, glycosylphosphatidylinositol; PI-PLC, phosphatidylinositol-specific phospholipase C; PNGase F, peptide *N*-glycosidase F; IT-MS, ion trap mass spectrometer; FT ICR-MS, Fourier transform ion cyclotron resonance mass spectrometer; GCC, graphitized carbon column; TIC, total ion chromatogram; CID, collision-induced dissociation; SIM, selected ion monitoring; dHex, deoxyhexose; Hex, hexose; HexNAc, *N*-acetylhexosamine; Fuc, fucose; Man, mannose; Gal, galactose; GlcNAc, *N*-acetylglucosamine; GlcN, glucosamine; NeuAc, *N*-acetylneuraminic acid; EtNH₂, ethanolamine; Ino, inositol; BA-2, brain-specific sugar chain, GlcNAc β 1–2Man α 1–6(GlcNAc β 1–4)(GlcNAc β 1–2Man α 1–3)Man β 1–4GlcNAc β 1–4(Fuc α 1–6)GlcNAc; SDS–PAGE, sodium dodecyl sulfate–polyacrylamide gel electrophoresis.

LAMP (Q62813)	1:	VRSVD--FNR	GTDN¹² ITVRQG	DTAILRCVVE	DKNSKVAWLN ³⁸	RSGIIFAGHD	KWSLDPRVEL	EKRHALEYSI	RIQKVDVYDE	GSYTCSVQQTQ	HEPKTSQVYL		
OBCAM (P32736)	1:	GVP	VRSVDATFPK	AMDN¹⁷ ITVRQG	ESATLRCTID	DRVTRVAWLN ⁴³	RSTILYAGND	KWSDIPRVII	LVNTPQYSI	MIQNVDDVDE	GPYTCSVQTD	NHPKTSRVHL	
neurotrimin (Q62718)	1:	SGDATFPK	AMDN¹² ITVRQG	ESATLRCTID	NRVTRVAWLN ³⁸	RSTILYAGND	KWCLDPRVVL	LSNTQTQYSI	EIQNVDDVDE	GPYTCSVQTD	NHPKTSRVHL		
Kilon (Q9Z0J8)	1:	VDFP----WA	AVDN	MLVRKG	DTAVLRCYLE	DGASKGAWLN ²⁶	RSSIIIFAGGD	KWSVDPRVSI	STLNKRQDYSL	QIQNVDDVDD	GPYTCSVQQTQ	HTPRTMQVHL	
LAMP	99:	IVQVPPKISN ¹⁰⁸	ISSDVTVNEG	SN¹²⁰ VTLVCMAN	GRPEPVTWR	HLP--LGRF	EGEEEYLEIL	GITREQSGKY	ECKAANEVSS	ADVQKVK	VTV	NYPPITITESK	
OBCAM	104:	IVQVPPGIMN ¹¹²	ISSDITVNEI	SS	VTLCLAI	GRPEPTVWR	HLSVKEQGF	VSEDEYLEIS	DIKRDQSGEY	ECSALNDVAA	PDVRKVK	ITV	NYPPYISKAK
neurotrimin	99:	IVQVSPKIVE	ISSDISINEG	NN¹²⁰ ISLTCIAT	GRPEPTVWR	HISPK-AVGF	VSEDEYLEIQ	GITREQSGEY	ECSASNDVAA	PVRRVSN ¹⁸⁴	VTV	NYPPYISEAK	
Kilon	97:	TVQVPPKIYD	ISNDMTINEG	TN¹¹⁸ VTLTCLAT	GKPEPAISWR	HISPS-AKPF	ENGQ-YLDIY	GITRDQAGEY	ECSAENDVSF	PDVKKVR	VVV	NFAPTIQEI	
LAMP	198:	SNEATTGRQA	SLKCEASAVP	APDFEWYRDD	TRI-NSANGL	EIKS	TEGQSS	LTVTN ²²⁵ VTEEH	YGN²²⁹ YTCVAAN	KLGVN ²⁷² ASLV	LFRPGSV-RG	IN ¹⁹⁸	
OBCAM	204:	NTGVSQVQKQ	ILSCEASAVP	MAEFQWFKED	TRLATGLDGV	RIEN	KGRIST	LTFN ²²⁶ VSEKD	YGN²²⁶ YTCVATN	KLGN ²⁷² ASIT	LYGPGAVIDG	VN ¹⁹⁸	
neurotrimin	198:	GTGVFVQKQ	TLQCEASAVP	SAEFQWFKDD	KRLVEGKGV	KVEN	RPFLSR	LTFN ²²⁵ VSEHD	YGN²²⁰ YTCVASN	KLGH ²⁷³ ASIM	LFGPGAVSEV	NN ¹⁹⁸	
Kilon	195:	SGVTIPGRSG	LIRCEGAGVP	PPAFEWYKGE	KRLFNGQGI	IIQN ²³⁸ FSTRSI	LTVTN ²⁴⁹ VTOEH	FGN²²⁷ YTCVAAN	KLGTN ²⁷⁰ ASLP	LNPSTAQYG	ITG ¹⁹⁵		

FIGURE 1: Amino acid sequence and potential N-glycosylation sites (in bold) of IgLON family proteins. Their accession numbers in Swiss-prot database are shown in parentheses after their names. The C-terminal amino acids in the proteins are predicted GPI attachment sites.

these proteins are distributed differently in the central nervous system during the development of neurons in a brain (11, 13–18). The IgLON family proteins consist of three Ig domains, the third of which is attached to a glycosylphosphatidylinositol (GPI) anchor. Each of the IgLON family proteins includes six or seven consensus N-glycosylation sites (Figure 1), and the glycosylation is presumed to play essential roles in the neural circuit formation like other Ig superfamily proteins (2–4). However, since the high degree of homology of their amino acid sequences makes it difficult to isolate the individual proteins of this family to perform carbohydrate analysis, their glycosylation features are still unknown with the exception of a linkage of N-glycans in OBCAM and Kilon and of high mannose-type and hybrid-type oligosaccharides in LAMP (9, 18, 19).

Recently, liquid chromatography and mass spectrometry (LC–MS) and liquid chromatography and multiple-stage mass spectrometry (LC–MSⁿ) have been widely applied to the site-specific glycosylation analysis of a glycoprotein (20–24). Generally, a tryptic digest of an isolated glycoprotein is separated with a reversed-phase or normal-phase column, and the separated glycopeptides are directly subjected to MS and MSⁿ (25–27). The site-specific glycosylation is deduced from the mass spectra of the glycopeptides, and the sequences of both the peptide and carbohydrate portions are deduced from the fragment ions in the MSⁿ spectra. Using this technique, we previously performed a site-specific glycosylation analysis of rat brain Thy-1, which contains three N-glycosylation sites and a GPI anchor (28). GPI-anchored proteins enriched via phase partitioning with Triton X-114 and PIPLC digestion were separated by SDS–PAGE, and the Thy-1 protein extracted from the gel was digested with trypsin or endoproteinase Asp-N. The Thy-1 glycopeptides were separated and analyzed by using a liquid chromatography and ion trap mass spectrometer (IT-MS) equipped with a C18 column. The peptide portions of glycopeptides were identified on the basis of the *m/z* values of the peptide-related ions and the b- and y-ions that arose from the peptide backbone. The carbohydrate structures at each glycosylation site and in the GPI moiety were successfully determined from fragment ions in the MS/MS spectra. This result suggests that LC–MSⁿ can be effectively utilized for site-specific glycosylation analysis of each glycoprotein in the mixture of several glycoproteins simultaneously.

In this study, we conducted site-specific glycosylation analyses of rat LAMP, OBCAM, neurotrimin, and Kilon using LC–MSⁿ. The GPI-linked proteins in the rat brains were separated by SDS–PAGE, and the IgLON family proteins were extracted from a gel band (45–70 kDa). The

mixture of proteins was digested with proteinases, and the site-specific glycosylation analysis of the four proteins was performed by using an ion trap-Fourier transform ion cyclotron resonance mass spectrometer (IT-MS-FT ICR-MS), which is capable of acquiring the accurate mass as well as the MSⁿ spectra. We successfully elucidated the site-specific glycosylation and the structure of the GPI moieties of LAMP, OBCAM, neurotrimin, and Kilon. This is the first report of the simultaneous site-specific glycosylation analysis of four similar glycoproteins.

EXPERIMENTAL PROCEDURES

Materials. The rat brains (Wister, male, 3 weeks old) were purchased from Nippon SLC (Hamamatsu, Japan). Phosphatidylinositol-specific phospholipase C (PIPLC) from *Bacillus cereus* was obtained from Molecular Probes (Eugene, OR). Trypsin-Gold was purchased from Promega (Madison, WI). PNGase F and endoproteinase Glu-C were purchased from Roche Diagnostics (Mannheim, Germany). SimplyBlue SafeStain was obtained from Invitrogen (Carlsbad, CA). All other chemicals were of the highest available purity.

SDS–PAGE of Enriched Lipid-Free GPI-Linked Proteins. Lipid-free GPI-linked proteins were enriched from rat brain as reported previously (28, 29). Briefly, the homogenate of two rat brains (total wet weight of 1.4 g) was defatted and solubilized with 2% Triton X-114 at 4 °C overnight (29, 30). After centrifugation, the supernatant was subjected to Triton X-114 phase partitioning at 37 °C. Cold acetone was added to the detergent phase containing solubilized membrane proteins, and the resulting precipitate was digested with PIPLC. After the PIPLC digest mixture had been subjected to Triton X-114 phase partitioning, lipid-free GPI-linked proteins in the aqueous phase were precipitated via addition of cold acetone. These proteins were separated by SDS–PAGE (12.5%) (brain wet weight of 50 mg/lane) after carboxyamidomethylation (31) and detected after being stained with Coomassie Brilliant Blue G-250 using SimplyBlue SafeStain.

Protein Identification. Gel-separated proteins were extracted after in-gel trypsin digestion as previously reported (32) and subjected to LC–MS/MS with a Paradigm MS4 HPLC system (Michrom BioResources, Inc., Auburn, CA) consisting of pump A with 0.1% formic acid and 2% acetonitrile and pump B with 0.1% formic acid and 90% acetonitrile. Peptides were separated with a Magic C18 column (50 mm × 0.2 mm, 3 μm; Michrom BioResources Inc.) with a linear gradient from 5 to 65% of pump B over

20 min at a flow rate of 3 $\mu\text{L}/\text{min}$. Mass spectra were recorded with a Finnigan LTQ system (Thermo Fisher Scientific, Waltham, MA) using sequential scan events: MS (m/z 450–2000) followed by data-dependent MS/MS on the IT-MS for the most intense ions in positive ion mode. For protein identification, all obtained product ions were subjected to a computer database search analysis with the TurboSEQUENT search engine (Thermo Fisher Scientific) using the Swiss-Prot database and search parameters: a static modification of carboxyamidomethylation (57 Da) at Cys and trypsin for digestion.

Extraction and Proteinase Digestion of the 45–70 kDa Proteins Separated by SDS–PAGE. The gel-separated proteins were extracted as previously reported (28). The proteins were extracted with 20 mM Tris-HCl containing 1% SDS by being shaken vigorously overnight after the gel had been broken down into small bits. The extract was filtered with Ultrafree-MC (0.22 μm ; Millipore, Bedford, MA), and the proteins were precipitated via addition of cold acetone. The resulting precipitate was digested with endoproteinase Glu-C (3.75 μg) in 30 μL of 0.1 M ammonium acetate (pH 8.0) at 37 $^{\circ}\text{C}$ for 4 days, followed by incubation with additional trypsin (1 μg) at 37 $^{\circ}\text{C}$ overnight.

LC–MSⁿ. Proteolytic peptides were separated by reversed-phase columns, Magic C30 and C18 (50 mm \times 0.1 mm, 3 μm ; Michrom BioResources), and a graphitized carbon column (GCC), Hypercarb 5 μ (150 mm \times 0.2 mm; Thermo Fisher Scientific), with a Paradigm MS4 HPLC system consisting of pump A with 0.1% formic acid and 2% acetonitrile and pump B with 0.1% formic acid and 90% acetonitrile. For analysis of glycopeptides, separation was performed with a linear gradient from 5 to 50% pump B over 100 min followed by a 50 to 95% B gradient over 10 min and 95% B over 10 min at a flow rate of 0.5 $\mu\text{L}/\text{min}$, and mass spectra were recorded with a Finnigan LTQ-FT system (Thermo Fisher Scientific) using sequential scan events: MS (m/z 1000–2000 or 700–2000) with the IT-MS followed by MS with the IT-MS-FT ICR-MS in selected ion monitoring (SIM) mode and data-dependent MSⁿ with the IT-MS for the most intense ions. The LC–MSⁿ runs were performed with a C30 column and scan range of m/z 1000–2000 (condition A), twice, with a C30 column and scan range of m/z 700–2000 (condition B), once, and with a C18 column and scan range of m/z 1000–2000 (condition C), once. For analysis of GPI-linked peptides, separation was performed with a linear gradient from 5 to 60% pump B over 100 min at a flow rate of 2 $\mu\text{L}/\text{min}$ for a GCC, and mass spectra were recorded with a Finnigan LTQ system using sequential scans: a single mass scan (m/z 700–2000) with the IT-MS followed by data-dependent MSⁿ scans with the IT-MS for the most intense ions, twice. LC–MSⁿ was performed using a capillary voltage of 1.8 kV and a capillary temperature of 200 $^{\circ}\text{C}$.

RESULTS

Preparation of Lipid-Free IgLON Glycopeptides. Figure 2 illustrates the experimental procedure for the glycosylation analysis of IgLON family proteins. Lipid-free GPI-linked proteins in a rat brain tissue sample were enriched via phase partitioning with Triton X-114 and PIPLC digestion. The enriched proteins were separated by SDS–PAGE and stained

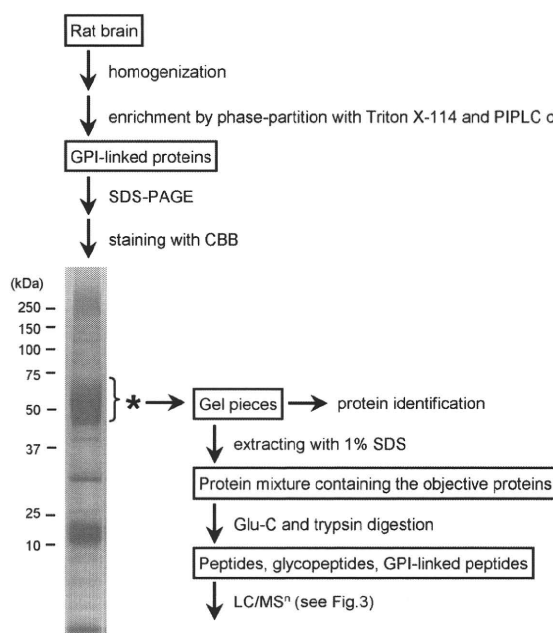


FIGURE 2: Experimental procedure for site-specific glycosylation analysis of IgLON family proteins and SDS–PAGE (12.5%) of lipid-free GPI-linked proteins which were enriched from rat brain. The asterisk indicates the gel band containing IgLON family proteins.

with Coomassie Brilliant Blue. The presence of LAMP, OBCAM, neurotrimin, and Kilon in the gel band at 45–70 kDa was confirmed by in-gel trypsin digestion followed by LC–MS/MS. The IgLON proteins were extracted with other comigrated proteins from 45–70 kDa bands in other lanes by being shaken in 1% SDS. After SDS had been removed, the mixture of proteins was digested with endoproteinase Glu-C and trypsin. Most of the resulting glycopeptides contained only a single N-glycosylation site, with the exception of LGTTN²⁷⁰ASLPLNPPSTAQYGITG²⁸⁷ in Kilon, which included a predicted GPI attachment site at Gly287 in addition to a potential N-glycosylation site at Asn270 (Figure 1). The glycopeptides from IgLON family proteins was separated by using three different columns: a reversed-phase column, a C30 and a C18 column for hydrophobic glycopeptides, and a GCC for hydrophilic glycopeptides, including GPI-linked peptides.

Glycosylation Analysis of LAMP. LC–MS analysis was performed via MS on the IT-MS and data-dependent MS in SIM mode on the FT ICR-MS, and data-dependent MS/MS and MS/MS/MS were performed on the IT-MS in the positive ion mode (Figure 3). After MS data acquisition, the MS/MS spectrum (scan n) of a glycopeptide was selected manually from all MS data on the basis of the existence of carbohydrate distinctive fragments, such as Hex₁HexNAc₁⁺ (m/z 366) and Hex₁HexNAc₁NeuAc⁺ (m/z 657). Then a set of the glycopeptide's MS data consisting of the mass spectrum (scan $n - 2$), the mass spectrum in SIM on the FT ICR-MS (scan $n - 1$), the MS/MS spectrum (scan n), and the MS/MS/MS spectrum (scan $n + 1$) was selected from all the MS data (step 1). The carbohydrate structure was deduced from the fragment ions appearing in the MS/MS spectrum (scan n), and the peptide portion was estimated from the peptide-related ions (step 2). The sequences of some peptides were confirmed by the b- and y-ions that arose from Y₁ ([peptide + HexNAc + H]⁺) in MS/MS/MS (scan $n +$

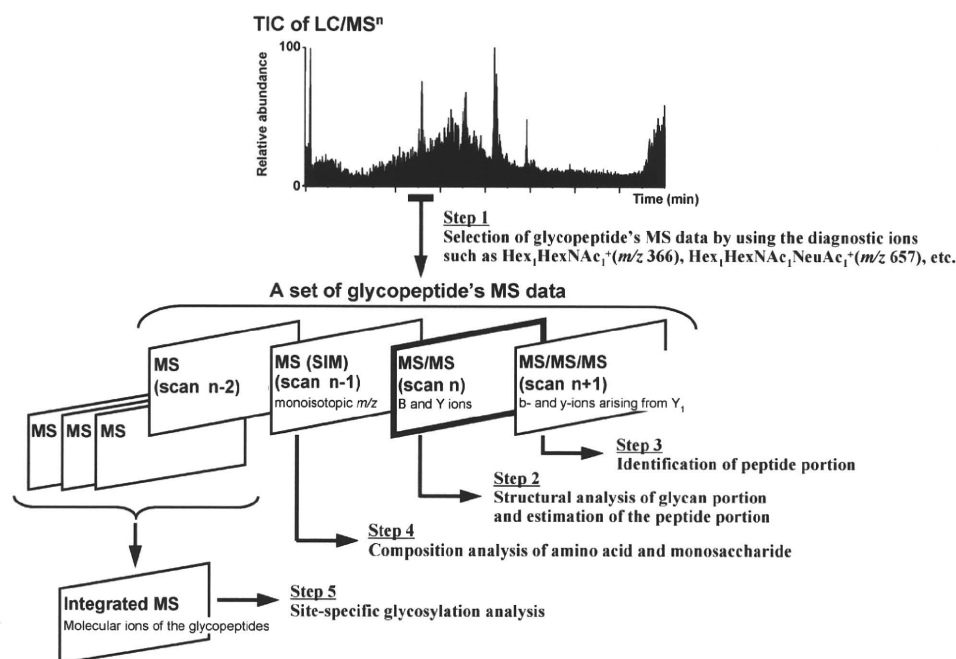


FIGURE 3: Methods used for LC-MSⁿ and data analysis.

1) (step 3). The accurate molecular mass that was calculated from the monoisotopic *m/z* value and the charge state acquired by FT ICR-MS in SIM mode (scan $n - 1$) was used to corroborate the assignment of the peptide and glycan moieties (step 4). The mass spectra acquired at the elution position, where the glycopeptides that yielded identical Y_1 ions in the MS/MS and/or MS/MS/MS spectra, were integrated, and the site-specific glycosylation was elucidated on the basis of the distribution of molecular ions in the integrated mass spectra (step 5). As a representative separation pattern, a total ion chromatogram (TIC) obtained by LC-MSⁿ with a C30 column (scan range of *m/z* 1000–2000) is shown in Figure 4A. The MS/MS spectra containing the diagnostic ions at *m/z* 366 and 657 were picked out from all the MS data, and the peptides eluted at positions 1–25 were determined to be the glycopeptides on the basis of the carbohydrate-related ions. The 19% of spectra acquired at elution time, including positions 1–25, could be traced back to the glycopeptides of IgLON family proteins.

As for LAMP, it has seven potential N-glycosylation sites at Asn12, -38, -108, -120, -251, -259, and -272, and Asn287 is the predicted site of GPI linkage. On the basis of the presence of the peptide-related ions ($[\text{peptide} + \text{HexNAc} + \text{H}]^+$, Y_1 or $Y_{1\alpha/1\beta}$; or $[\text{peptide} + \text{dHex-HexNAc} + \text{H}]^+$, $Y_{1\alpha}$), glycopeptides that were eluted at the positions 1, 11, 14, 12, 4, and 24 were estimated to be the glycopeptides containing Asn12, -38, -108, -251, -259, and -272, respectively. The MS/MS spectra of the glycopeptide containing Asn120 (GSN¹²⁰VTLCMANGRPE) were not acquired in any of the runs. However, glycosylation at Asn120 was confirmed by the detection of the peptide substituted with Asp (GSD¹²⁰VTLCMANGRPEPVITWR) after PNGase F digestion (data not shown). Panels A1–F1 of Figure 5 show the representative MS/MS and MS/MS/MS spectra acquired at positions 11, 1, 14, 12, 4, and 24, respectively. The integrated mass spectra of the glycopeptides containing Asn38, -12, -108, -251, -259, and -272 are shown in panels A2–F2 of Figure 5, respectively. The feature of the

glycosylation at each glycosylation site was elucidated on the basis of these MS spectra.

(i) *Asn38* (*Asn43* in OBCAM and *Asn38* in neurotrimin). Panel A1 of Figure 5 shows one of the MS/MS spectra acquired at position 11. The peptide portion, VAWL(GlcNAc)₁N³⁸R, was confirmed on the basis of the *b*- and *y*-ions that arose from Y_1 (*m/z* 961.5) in the MS/MS/MS spectrum (panel A1'' of Figure 5). A series of doubly charged *Y* ions with an *m/z* spacing pattern, 81 *m/z* units (Hex), suggests the linkage of Man-7 to this peptide. The attachment of Man-7 to VAWLN³⁸R, whose theoretical monoisotopic *m/z* value ($[\text{M} + 2\text{H}]^{2+}$) is 1149.983, was ascertained by the observed monoisotopic *m/z* value (1149.986) acquired in SIM mode on the FT ICR-MS (panel A1' of Figure 5). Panel A2 of Figure 5 shows the integrated mass spectrum which was obtained from the mass spectra of glycopeptides that yielded Y_1 (*m/z* 961.5) via MS/MS. Four noticeable ion peaks (peaks a-1–a-4) appearing with the differences of 81 *m/z* units are assigned to VAWLN³⁸R glycosylated with Man-6-9 (Table 1A). The MS/MS spectra of DKNSKVAWLN³⁸R and CVVEDKNSKVAWLN³⁸R, which were picked out from positions 9 and 15, also revealed that Man-5, -7, and -8 were attached to Asn38.

(ii) *Asn12*. Panel B1 of Figure 5 shows the representative MS/MS spectrum of glycopeptide, GTDN¹²ITVR, which was selected from position 1. From the $Y_{1\alpha}$ ion (*m/z* 1224.5) together with monoisotopic *m/z* value of the molecular ion (*m/z* 1173.132) and a series of doubly charged *Y* ions with an *m/z* spacing pattern, 146 (NeuAc), 101 (HexNAc), and 81 *m/z* units (Hex), the carbohydrate portion was estimated to be dHex₁Hex₅HexNAc₄NeuAc₄. Furthermore, a complex-type oligosaccharide, to which one branch of disialic acid was attached, was deduced from the presence of $B_{4\alpha}/Y_{5\alpha'}$ (*m/z* 495.3), $B_{2\alpha}$ (*m/z* 582.7), $B_{3\alpha}$ (*m/z* 744.9), $B_{4\alpha}/Y_{5\alpha''}$ and $B_{4\alpha}/Y_{7\alpha'}$ (*m/z* 948.2), and $B_{4\alpha}$ (*m/z* 1239.5) (inset of panel B1 of Figure 5). The integrated mass spectrum at position 1 suggests that the majority of the glycans at Asn12 are hybrid- and complex-type oligosaccharides containing disialic acids

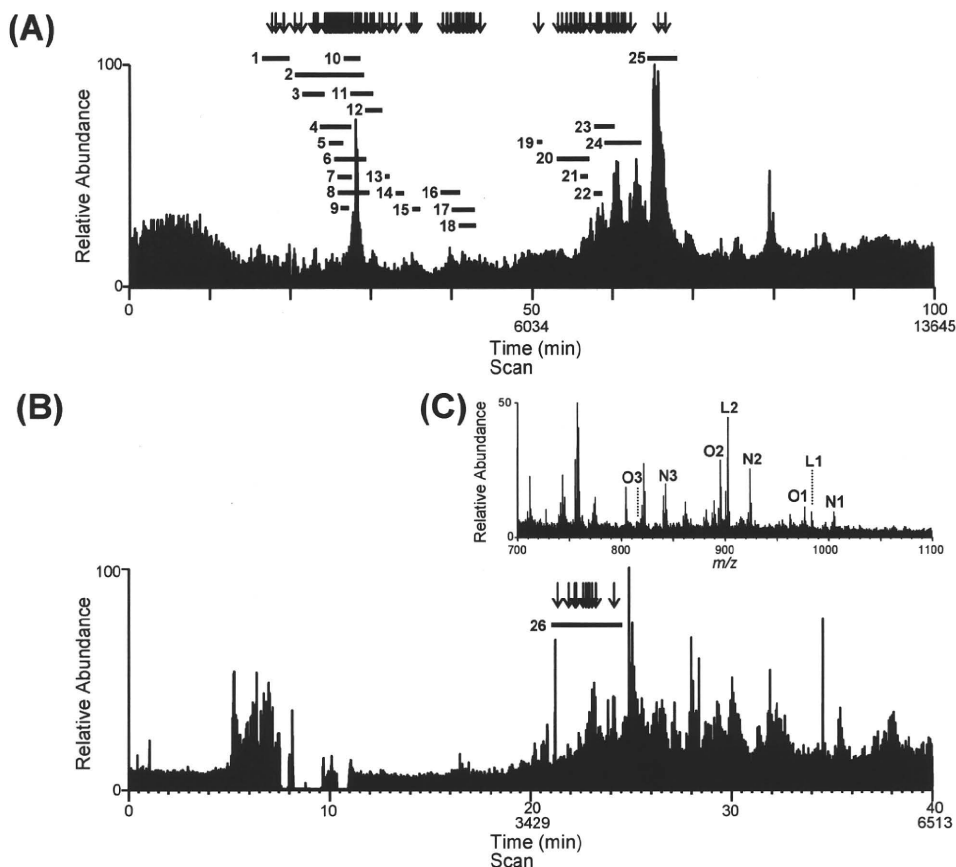


FIGURE 4: Total ion chromatograms obtained by C30-LC-MSⁿ (A) and GCC-LC-MSⁿ (B). Lines 1–25 and 26 are the elution positions of glycopeptides and GPI-linked peptides, respectively. The down arrow denotes the extracted position of the MS/MS spectra. (C) Integrated mass spectrum obtained from elution position 26. L1 and L2 are molecular ions of GPI-linked peptides from LAMP, N1–N3 those from neurotrimin, and O1–O3 those from OBCAM.

(panel B2 of Figure 5 and Table 1B). In addition, the partial glycosylation at Asn12 was indicated by the detection of nonglycosylated GTDN¹²ITVR.

(iii) *Asn108*. The MS/MS spectrum of glycosylated ISN¹⁰⁸ISSDVTVNE ($Y_{1\alpha/1\beta}$, m/z 1480.6) acquired at position 14 is shown in panel C1 of Figure 5. The attachment of a Lewis *a/x* [$Le^{a/x}$, Gal-(Fuc-)GlcNAc-] or H antigen (Fuc-Gal-GlcNAc-) motif to the bisected complex-type oligosaccharide was deduced from the monosaccharide composition (dHex₂Hex₄HexNAc₅) and the $Le^{a/x}$ and H antigen-related ion (m/z 512.1) and $Y_{1\beta/3\alpha/3\beta}^{2+}$ (m/z 1024.3) (panel C1 of Figure 5, peak c-1 in panel C2 of Figure 5). The alternative LC-MSⁿ run with the C30 column (scan range of m/z 1000–2000) suggested that ISN¹⁰⁸ISSD is also occupied by sialyl $Le^{a/x}$ (s $Le^{a/x}$)-modified or core-fucosylated hybrid-type oligosaccharides based on the presence of NeuAc-Hex-(dHex-)-HexNAc⁺ (m/z 803.1), Hex-(dHex-)-HexNAc⁺ (m/z 512.3), NeuAc-Hex⁺ (m/z 454.2), and [peptide + dHex + HexNAc + H]⁺ (m/z 1084.3) (data not shown, Table 1C).

(iv) *Asn251*. The representative MS/MS spectrum of the glycopeptide containing GQSSLTVTN²⁵¹VTE ($Y_{1\alpha/1\beta}$, m/z 1438.6; elution position 12) is shown in panel D1 of Figure 5. From the monoisotopic mass and the $Le^{a/x}$ -related ions (m/z 350.3 and 512.2), the carbohydrate structure was estimated to be a complex-type oligosaccharide to which the $Le^{a/x}$ motif was attached (dHex₂Hex₄HexNAc₅; inset of panel D1 of Figure 5). Other glycans at Asn251 were characterized as complex-type oligosaccharides containing s $Le^{a/x}$ or Lewis b/y [$Le^{b/y}$, Fuc-Gal-(Fuc-)GlcNAc-] based on the molecular

ions in the integrated mass spectrum (peaks d-1–6 in panel D2 of Figure 5), the s $Le^{a/x}$ -related ions (m/z 803, 657, and 512), and the $Le^{b/y}$ -related ions (m/z 658.2, 512.1, and 350.2) acquired by the alternative run with the C30 column (scan range of m/z 700–2000) (Table 1D).

(v) *Asn259*. Panel E1 of Figure 5 shows the product ion spectra of HYGN²⁵⁹YTCVAANK linked by dHex₁Hex₃-HexNAc₅, which was deduced from the $Y_{1\alpha/1\beta}$ ion (m/z 1600.6) and the monoisotopic mass acquired at position 4. The BA-2, which is a core-fucosylated and agalactobiantennary oligosaccharide with bisecting GlcNAc, and known as a brain-specific carbohydrate, was suggested by the product ions at m/z 1085.3 (bisecting GlcNAc) and 1746.6 (core-fucosylation) (inset of panel E1 of Figure 5). The majority of other glycans at Asn259 were characterized as $Le^{a/x}$ -modified complex and hybrid types. Man-5 was suggested to be a minor glycan (panel E2 of Figure 5 and Table 1E).

(vi) *Asn272*. Panel F1 of Figure 5 shows the MS/MS and MS/MS/MS spectra of glycopeptide LGVTN²⁷²ASLVLFVR ($Y_{1\alpha/1\beta}$, m/z 1492.8), which were acquired at position 24. The monosaccharide composition (dHex₂Hex₄HexNAc₅) and the presence of $Y_{3\alpha/3\beta}^{2+}$ (m/z 1103.8) and $Le^{a/x}$ -related ion suggested the attachment of a $Le^{a/x}$ or H antigen motif to the bisected and core-fucosylated complex-type oligosaccharide (inset of panel F1 of Figure 5). The MS/MS spectra of the LGVTN²⁷²ASLVLFVRPGSVR glycopeptides ($Y_{1\alpha/1\beta}^{2+}$, m/z 1069) were also picked out at position 24 (data not shown). The m/z values of molecular ions appearing in the

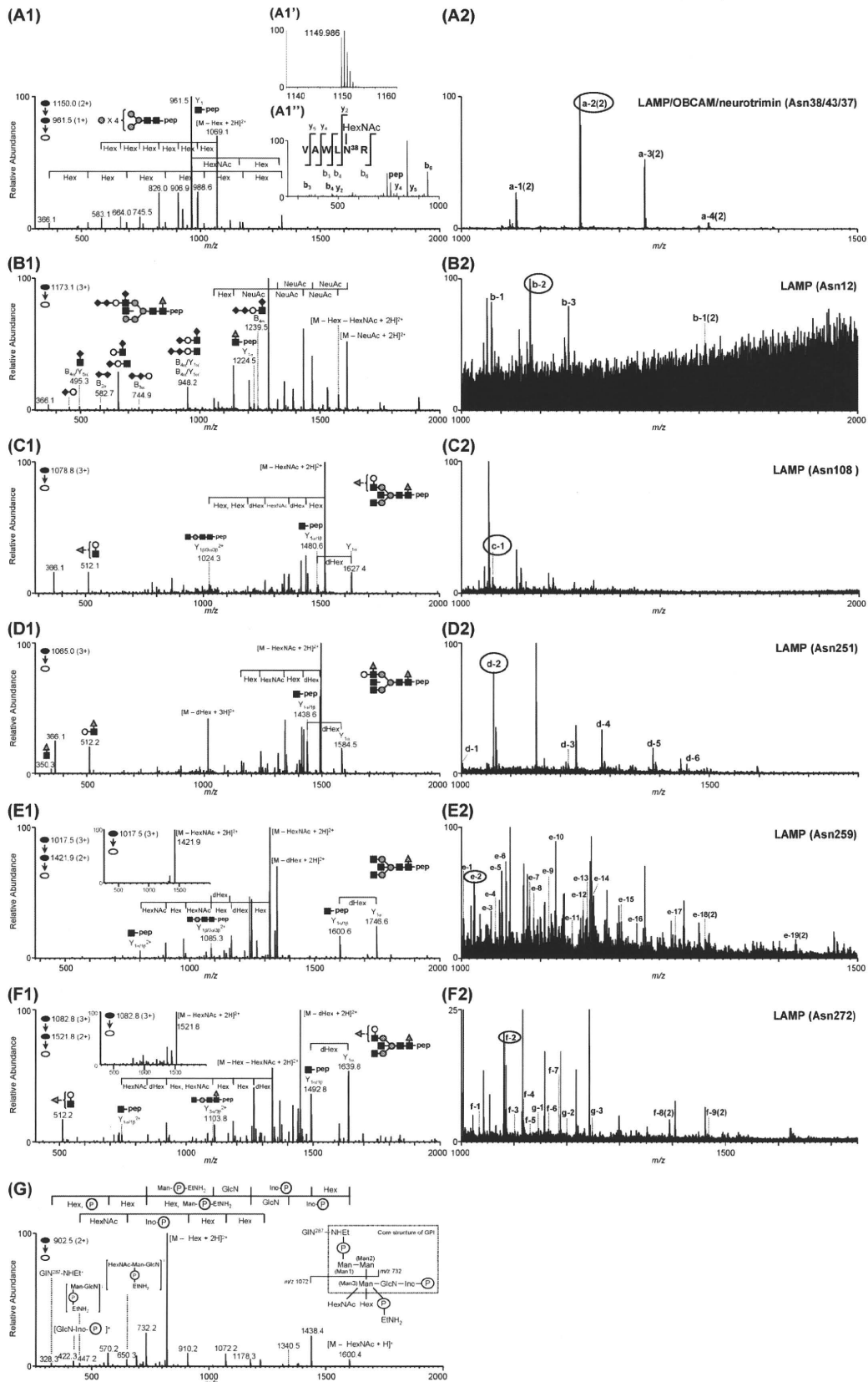


FIGURE 5: MS spectra of LAMP glycopeptides. (A1) MS/MS spectrum of glycopeptide VAWLN³⁸R; elution position, 11; precursor ion, [M + 2H]²⁺ (*m/z* 1150.0). (A1') Mass spectrum on the FT ICR-MS in SIM mode. (A1'') MS/MS/MS spectrum acquired from Y₁ (*m/z* 961.5). (A2) Integrated mass spectrum obtained from position 11. (B1) MS/MS spectrum of glycopeptide GTDN¹²¹TVTR; elution position, 1; precursor ion, [M + 3H]³⁺ (*m/z* 1173.1). (B2) Integrated mass spectrum at position 1. (C1) MS/MS spectrum of glycopeptide ISN¹⁰⁸ISSDVTVNE; elution position, 14; precursor ion, [M + 3H]³⁺ (*m/z* 1078.8). (C2) Integrated mass spectrum at position 14. (D1) MS/MS spectrum of glycopeptide GQSSLTVTN²⁵¹VTE; elution position, 12; precursor ion, [M + 3H]³⁺ (*m/z* 1065.0). (D2) Integrated mass spectrum at position 12. (E1) MS/MS and MS/MS/MS spectra of glycopeptide HYGN²⁵⁹YTCVAANK; elution position, 4; precursor ion, [M + 3H]³⁺ (*m/z* 1017.5). (E2) Integrated mass spectrum at position 4. (F1) MS/MS and MS/MS/MS spectra of glycopeptide LGVTN²⁷²ASLVLFRR; elution position, 24; precursor ion, [M + 3H]³⁺ (*m/z* 1082.8). (F2) Integrated mass spectrum at position 24. (G) MS/MS spectrum of GPI-linked GIN²⁸⁷; elution position, 26; precursor ion, [M + 2H]²⁺ (*m/z* 902.5). Symbols are as in Figure 9.

Table 1: Summary of Glycosylation Analysis of IgLON Family Proteins

protein	peptides				glycopeptides				N-glycan				
	sequence ^{a,b}	elution position	Figure	peak no. ^c	scan in Figure 4A ^d	observed peptide-related ion ^e	observed m/z in SIM mode ^b	theoretical m/z ^b	deduced monosaccharide composition				
									dHex	Hex	HexNAc	NA	deduced structure ^f (diagnostic ion)
LAMP	B GTDN ¹² ITVR (874,451)	1	5, B2	b-1	2095 (A, B)	1225.4	1076.101 (3)	1076.101	1	5	4	2	H, CoreF(1225.4)
									1	5	4	2	H, CoreF(1225.6)
									1	5	4	3	H, CoreF(1224.5), diSia(582.7) [Figure 5, B1]
									1	5	4	3	CoreF(1224.5), diSia(583.0)
									1	5	4	4	C, CoreF(1224.5), diSia(583.0)
									1	5	4	5	C, CoreF(1225.6), diSia(583.4)
									0	5	2	0	Man-5
									0	6	2	0	Man-6
									0	7	2	0	Man-7 [Figure 5, A1]
									0	8	2	0	Man-8
A	V A W L N ³⁸ R (757,424)	11	5, A2	a-1 (2)	3523 (A, B, C)	961.5	987.930 (2)	987.930	0	5	2	0	Man-5
									0	6	2	0	Man-6
									0	7	2	0	Man-7 [Figure 5, A1]
									0	8	2	0	Man-8
									0	9	2	0	Man-9
									0	10	2	0	Man-10
									0	11	2	0	Man-11
									0	12	2	0	Man-12
									0	13	2	0	Man-13
									0	14	2	0	Man-14
C	I S N ¹⁰⁸ I S S D (734,345)	-	-	-	-	938.4	1296.508 (2)	1296.507	1	5	3	1	H, CoreF(1084.3) or sL ^{u,k} (454.2, 512.3, 657.2, 803.1)
									1	6	3	1	H, CoreF(1084.2)
									2	4	5	0	C, CoreF(1627.4), bisectGN(1024.3) [Figure 5, C1] glycosylated ^g
									1	3	4	0	CoreF(1584.6), bisectGN(1003.6)
									1	3	5	0	C, CoreF(1584.5), bisectGN(1004.1), BA-2
									1	3	5	0	C, CoreF(1584.5), bisectGN(1077.2), BA-2
									1	5	4	0	H, CoreF(1584.5) or L ^{u,k} (350.1, 512.1)
									2	4	5	0	C, CoreF(1584.5), L ^{u,k} (350.3, 512.2) [Figure 5, D1]
									2	4	5	0	C, CoreF(1585.6), 512(512.2)
									3	5	5	0	C, CoreF(1584.5), bisectGN(1004.1), L ^{b,y} (350.2, 512.1, 658.2)
D	G S N ¹²⁰ V T L V C M A N G R P E P V I T W R (1603,745)	12	5, D2	d-1	3630	1438.5	1002.088 (3)	1002.088	1	5	4	0	H, CoreF(1584.5) or L ^{u,k} (350.1, 512.1)
									2	4	5	0	C, CoreF(1585.6), 512(512.2)
									3	5	5	0	C, CoreF(1584.5), bisectGN(1004.1), L ^{b,y} (350.2, 512.1, 658.2)
									2	5	5	1	C, CoreF(1584.4), 512(512.3)
									2	5	6	1	C, CoreF(1584.5) (sL ^{u,k} (512.2, 657.2, 803.2))
									3	6	6	1	C, CoreF(1584.5) (sL ^{u,k} (512.2, 657.3, 803.1))
									3	6	7	1	C, CoreF(1584.6), 512(512.2)
									2	4	5	0	C, CoreF(1585.6), 512(512.2)
									3	5	5	0	C, CoreF(1584.5), bisectGN(1004.1), L ^{b,y} (350.2, 512.1, 658.2)
									2	5	5	1	C, CoreF(1584.4), 512(512.3)
D	G O S S L T V T N ²⁵ I V T E (1234,604)	12	5, D2	d-2	3646 (A, B, C)	1438.6	1064.451 (3)	1064.450	2	4	5	0	C, CoreF(1584.5), L ^{u,k} (350.3, 512.2) [Figure 5, D1]
									2	4	5	0	C, CoreF(1585.6), 512(512.2)
									3	5	5	0	C, CoreF(1584.5), bisectGN(1004.1), L ^{b,y} (350.2, 512.1, 658.2)
									2	5	5	1	C, CoreF(1584.4), 512(512.3)
									2	5	6	1	C, CoreF(1584.5) (sL ^{u,k} (512.2, 657.2, 803.2))
									3	6	6	1	C, CoreF(1584.5) (sL ^{u,k} (512.2, 657.3, 803.1))
									3	6	7	1	C, CoreF(1584.6), 512(512.2)
									2	4	5	0	C, CoreF(1585.6), 512(512.2)
									3	5	5	0	C, CoreF(1584.5), bisectGN(1004.1), L ^{b,y} (350.2, 512.1, 658.2)
									2	5	5	1	C, CoreF(1584.4), 512(512.3)

Table 1: Continued

protein	sequence ^{a,b}	peptides				glycopeptides							N-glycan				
		elution position	Figure	peak no. ^c	scan in Figure 4A ^d	observed peptide-related ion ^e	observed <i>m/z</i> in SIM mode ^b	theoretical <i>m/z</i> ^b	deduced monosaccharide composition			N-glycan					
									dHex	Hex	HexNAc	NA	Man-5	deduced structure ^f (diagnostic ion)			
E	HYGN ²⁵⁹ YTCVAANK (1396.619)	4	5, E2		— (B)	801.8(2)	872.021 (3)	872.021	0	5	2	0	0	Man-5			
				e-18 (2)	2884	1600.6	1307.532 (2)	1307.528	0	5	2	0	0	Man-5	CoreF(1746.7), bisectGN(1085.6)		
				e-19 (2)	2949 (A)	1601.4	1421.587 (2)	1421.584	1	3	4	0	0	CoreF(1746.6), bisectGN(1085.3)			
				e-1	2891 (A, C)	1600.6	1002.079 (3)	1002.076	1	4	4	0	0	C, CoreF(1746.6), bisectGN(1085.3), BA-2 [Figure 5, E1]			
				e-2	2931 (A, B, C)	1600.6	1015.752 (3)	1015.752	1	3	5	0	0	H, CoreF(1746.6), 512(512.1)			
				e-3	2859 (A)	1600.5	1037.089 (3)	1037.086	2	5	3	0	0	H, 512(512.1)			
				e-4	2840	1600.6	1042.419 (3)	1042.418	1	6	3	0	0	CoreF(1746.6), L ^{ax} (350.2), bisectGN(1085.5)			
				e-5	2878 (A)	1601.6	1050.764 (3)	1050.762	2	4	4	0	0	H, CoreF(1747.7), bisectGN(1085.6)			
				e-6	2853 (A, B, C)	1600.5	1056.095 (3)	1056.094	1	5	4	0	0	H, CoreF(1747.6) or 512(512.2)			
				e-7	2994	1600.7	1085.433 (3)	1085.432	1	5	3	1	1	H, CoreF(1746.6), 512(512.2)			
				e-8	2821	1600.5	1091.107 (3)	1091.104	2	6	3	0	0	H, CoreF(1747.8), bisectGN(1158.7), L ^{ax} (349.9, 512.3)			
				e-9	2847	1600.6	1110.111 (3)	1110.111	1	6	4	0	0	H, CoreF(1746.6) or L ^{ax} (350.1, 512.3)			
				e-10	2898 (A, C)	1601.7	1118.457 (3)	1118.455	2	4	5	0	0	C, CoreF(1746.7), bisectGN(1085.7), L ^{ax} (350.2, 512.1)			
				e-11	2989	1600.7	1139.452 (3)	1139.450	1	6	3	1	1	H, CoreF(1746.7)			
				e-12	2808 (A)	1600.6	1153.467 (3)	1153.466	3	5	4	0	0	C, CoreF(1746.6), L ^{by} (658.2) or 512/512(512.1/512.3)			
				e-13	2872	1600.4	1158.798 (3)	1158.797	2	6	4	0	0	H, CoreF(1747.7), L ^{ax} (350.1, 512.1)			
				e-14	3036	1601.7	1166.800 (3)	1166.801	1	4	5	1	1	C, CoreF(1747.4) or 512(512.1), bisectGN(1085.3)			
				e-15	2983	1600.6	1201.813 (3)	1201.811	2	5	4	1	1	C, CoreF(1747.6), sL ^{ax} (350.1, 512.2, 657.3, 803.2)			
				e-16	2815	1600.6	1221.160 (3)	1221.159	3	5	5	0	0	C, CoreF(1747.6), bisectGN(1085.3), 512(512.2)			
				e-17	3013	1600.7	1269.507 (3)	1269.505	2	5	5	1	1	C, CoreF(1746.7), bisectGN(1085.5), 512(512.1)			

Table 1: Continued

protein	peptides		glycopeptides						N-glycan											
	sequence ^{a,b}	elution position	Figure	peak no. ^c	scan in Figure 4A ^d	observed peptide-related ion ^e	observed <i>m/z</i> in SIM mode ^b	theoretical <i>m/z</i> ^b	deduced monosaccharide composition											
									dHex	Hex	HexNAc	NA								
OBCAM	G AMDN ¹⁷² VTVR (904.444)	2	6, A2	h-1	2408 (A)	1254.5	1018.407 (3)	1018.405	2	5	5	1	C, CoreF(1639.1), sL ^{9A} (454.0, 512.6, 657.1, 803.0)							
									1	5	5	1	C, CoreF(1639.4), 512(512.3)							
									1	5	5	1	C, CoreF(1638.8) (sL ^{9A} (454.9, 512.3, 657.1, 803.3))							
									2	4	5	0	C, bisectGN(1279.5)							
									1	3	5	0	C, CoreF(1068.7), bisectGN(1352.3), BA-2							
									1	4	5	0	C, CoreF(1069.2) or 512(512.2)							
									2	4	5	0	C, CoreF(1068.4), bisectGN(1279.4), 512(512.2)							
									1	5	4	1	C, 512(512.2)							
									2	5	4	1	C, CoreF(1068.4), 512(512.3)							
									1	5	3	2	H, CoreF(1254.5), diSia(583.0)							
									1	5	4	2	CoreF(1254.7)							
									1	5	4	2	C, CoreF(1254.5)							
A	VAWLN ⁹³ R (757.424)	11	5, A2	2473 (A, B, C)	1254.5	1183.131 (3)	1183.130	1	5	4	3	H, CoreF(1254.5) or 512(512.2), diSia(582.6)								
								1	6	3	3	C, CoreF(1254.7), diSia(583.0)								
								1	5	4	4	C, CoreF(1254.5), diSia(582.9) [Figure 6, A1]								
								1	5	4	5	Man-5								
								0	5	2	0	Man-6								
								0	6	2	0	Man-7 [Figure 5, A1]								
								0	7	2	0	Man-8								
								0	8	2	0	Man-9								
								0	9	2	0	glycosylated ^g								
								0	0	0	0	glycosylated ^g								
								H	ISTLTFN ⁵⁸ SVSE (1256.629)	25	6, B2	2719 (C)	1254.5	1280.163 (3)	1280.162	1	5	4	4	CoreF(1606.3), bisectGN(1087.8)
																1	5	4	4	C, CoreF(1606.5), bisectGN(1088.6), BA-2
1	5	4	4	C, CoreF(1606.5), bisectGN(1088.4), BA-2																
1	5	4	4																	

Table 1: Continued

protein	sequence ^{a,b}	elution position	Figure	peak no. ^c	glycopeptides			N-glycan					
					scan in Figure 4A ^c	observed peptide-related ion ^e	observed <i>m/z</i> in SIM mode ^b	theoretical <i>m/z</i> ^b	deduced monosaccharide composition				
									dHex	Hex	HexNAc	NA	deduced structure ^f (diagnostic ion)
I	YGN ²⁶⁶ YTCVATNK (1289.571)	7	6, C2		1461.7	1071.792 (3)	1071.792	2	4	5	0	C, CoreF(1606.5), L ^{ax} (350.1, 512.2) or L ^{by} (658.4)	
					1460.5	1607.183 (2)	1607.184	2	4	5	0	C, 512(512.3)	
					1460.5	1120.138 (3)	1120.137	1	4	5	1	C, CoreF(1606.5)	
					1460.5	1155.148 (3)	1155.148	2	5	4	1	C, CoreF(1606.6) (sL ^{ax} (349.2, 512.2, 804.1))	
					1460.5	1174.494 (3)	1174.495	3	5	5	0	C, CoreF(1606.5), L ^{by} (350.7, 512.3, 658.2)	
					1461.4	1187.831 (3)	1187.831	1	4	6	1	C, CoreF(1606.6) or sL ^{ax} (350.1, 512.5, 657.1, 803.1)	
					1460.5	1222.842 (3)	1222.841	2	5	5	1	C, CoreF(1606.5), sL ^{ax} (454.0, 512.2, 803.2)	
					1460.5	1290.538 (3)	1290.534	2	5	6	1	C, CoreF(1606.6) (sL^{ax} (454.2, 512.2, 657.1, 803.3) [Figure 6, B1])	
					1460.5	1393.239 (3)	1393.238	3	6	6	1	C, CoreF(1606.5), 512(512.2)	
					1493.6	1254.003 (2)	1254.004	0	5	2	0	Man-5	
					1493.6	1368.060 (2)	1368.060	1	3	4	0	CoreF(1639.6), bisectGN(1031.5)	
					1493.6	980.068 (3)	980.069	1	3	5	0	C, CoreF(1639.6), bisectGN(1032.2), BA-2	
					j-4 (2)	3156 (A, B, C)			1493.6	1469.602 (2)	1469.599	1	3
1493.6	1015.082 (3)	1015.079	2	4					4	0	CoreF(1639.5), L ^{ax} (350.2, 512.1), bisectGN(1105.1)		
j-1	3048 (A)			1494.6	1082.774 (3)	1082.772	2	4	5	0	C, CoreF(1640.5), L ^{ax} (350.4, 512.2), bisectGN(1105.9) [Figure 6, C1]		
j-2	3030			1493.6	1117.783 (3)	1117.783	3	5	4	0	H, CoreF(1639.5), L ^{by} (350.3, 512.1, 658.1)		
				1494.6	1185.478 (3)	1185.476	3	5	5	0	C, CoreF(1639.6), L ^{ax} (349.0, 512.1), bisectGN(1032.7)		
j-3	3024			1608.6	1311.517 (2)	1311.518	0	5	2	0	Man-5		
				1609.7	1018.412 (3)	1018.411	1	3	5	0	C, CoreF(1754.5), bisectGN(1089.6), BA-2		
6	KDYGN ²⁶⁶ YTCVATNK (1532.693)	6	-		1608.6	1527.113 (2)	1527.113	1	3	5	0	C, CoreF(1754.6), bisectGN(1089.1), BA-2	
					1608.6	1121.115 (3)	1121.115	2	4	5	0	C, CoreF(1754.7), L ^{ax} (350.3, 512.3)	
13	DYGN ²⁶⁶ YTCVATNK (1404.598)	13	-		1608.7	1156.125 (3)	1156.125	3	5	4	0	H, CoreF(1754.8), 512(512.2)	
					1736.7	1489.625 (2)	1489.621	1	3	4	0	CoreF(1882.8), bisectGN(1225.1)	
6	KDYGN ²⁶⁶ YTCVATNK (1532.693)	6	-		1737.8	1061.109 (3)	1061.109	1	3	5	0	C, CoreF(1884.9), bisectGN(1226.7), BA-2	
					1737.7	1150.141 (3)	1150.137	2	5	4	0	H, CoreF(1883.8), L ^{ax} (350.4, 512.2)	

protein	peptides				glycopeptides				N-glycan					
	sequence ^{c,b}	elution position	Figure	peak no. ^c	scan in Figure 4A ^c	observed peptide-related ion ^e	observed <i>m/z</i> in SIM mode ^b	theoretical <i>m/z</i> ^b	deduced monosaccharide composition					
									dHex	Hex	HexNAc	NA	deduced structure ^f (diagnostic ion)	
neurotrimin	J LGNTN ²⁷⁹ ASITLYGPGAVID (1774-910)	-	-	-	(C)	1736.5	1163.814 (3)	1163.813	2	4	5	0	C, CoreF(1882.7), bisectGN(1153.7), L ^{NA} (350.3, 512.2)	
						1737.6	1198.826 (3)	1198.823	3	5	4	0	C, CoreF(1884.7), L ^{NA} (350.1, 512.2)	
						1737.1	1212.160 (3)	1212.159	1	4	5	1	C, CoreF(1883.9), bisectGN(1226.3)	
						1737.0	1247.170 (3)	1247.169	2	5	4	1	CoreF(1882.8), sL ^{NA} (453.8, 512.2, 657.2, 803.2)	
						1978.7	1093.161 (3)	1093.162	0	3	5	0	C	
						1979.8	1141.848 (3)	1141.848	1	3	5	0	C, CoreF(1062.9), bisectGN(1273.8), BA-2	
						1254.5	1018.407 (3)	1018.405	1	5	3	2	H, CoreF(1254.5), diSia(583.0)	
						1254.7	1086.098 (3)	1086.099	1	5	4	2	CoreF(1254.7)	
						1254.5	1628.644 (2)	1628.644	1	5	4	2	C, CoreF(1254.5)	
						1254.7	1115.437 (3)	1115.437	1	5	3	3	H, CoreF(1254.7), diSia(583.0)	
neurotrimin	G AMDN ²⁴ VTVR (904.444)	2	6, A2	h-1	(A)	1254.5	1018.407 (3)	1018.405	1	5	3	2	H, CoreF(1254.5), diSia(583.0)	
						1254.6	1169.454 (3)	1169.455	1	6	3	3	H, CoreF(1254.6), diSia(583.0)	
						1254.5	1183.131 (3)	1183.130	1	5	4	3	H, CoreF(1254.5) or 512(512.2), diSia(582.6)	
						1254.5	1280.163 (3)	1280.162	1	5	4	4	C, CoreF(1254.5), diSia(582.9) [Figure 6, A1]	
						1108.6	1377.198 (3)	1377.194	1	5	4	5	Man-5	
						961.5	987.930 (2)	987.930	0	5	2	0	Man-6	
						961.5	1068.956 (2)	1068.957	0	6	2	0	Man-7 [Figure 5, A1]	
						961.5	1149.986(2)	1149.983	0	7	2	0	Man-8	
						961.5	1231.010 (2)	1231.010	0	8	2	0	Man-9	
						961.5	1312.039 (2)	1312.036	0	9	2	0	glycosylated ^g	
K	LTFN ²⁵⁹ VE (955.465)	20	7, A2	(A)	1159.4	1086.954 (2)	1086.951	0	5	2	0	Man-5		
					1159.4	1180.493 (2)	1180.494	1	4	3	0	CoreF(1305.5)		
					1159.4	1201.011 (2)	1201.007	1	3	4	0	CoreF(1305.4)		
					1159.5	1261.520 (2)	1261.520	1	5	3	0	H, CoreF(1305.3)		
					1159.4	1302.551 (2)	1302.546	1	3	5	0	C, CoreF(1305.3), bisectGN(864.6), BA-2		
					1159.5	1334.551 (2)	1334.549	2	5	3	0	H, CoreF(1305.3), 512(512.3)		
					1159.4	1355.062 (2)	1355.062	2	4	4	0	CoreF(1305.2), 512(512.4)		
					1159.5	1363.059 (2)	1363.060	1	5	4	0	H, bisectGN(864.4), CoreF(1305.4) or 512(511.9)		
					1160.4	1407.068 (2)	1407.068	1	5	3	1	H, CoreF(1306.4)		
					1159.8	1415.576 (2)	1415.575	2	6	3	0	H, CoreF(1305.3)		

Table 1: Continued

protein	sequence ^{a,b}	peptides				glycopeptides				N-glycan			
		elution position	Figure	peak no. ^c	scan in Figure 4A ^d	observed peptide-related ion ^e	observed <i>m/z</i> in SIM mode ^b	theoretical <i>m/z</i> ^b	deduced monosaccharide composition				
									dHex	Hex	HexNAc	NA	
					1159.4	957.728 (3)	957.728	2	5	4	0	H, CoreF(1305.7), L ^{ax} (350.3, 512.1)	
			k-8 (2)	6735 (A, B)	1159.3	1436.093 (2)	1436.089	2	5	4	0	H, CoreF(1305.4), 512(512.3)	
				— (A)	1159.7	1444.089 (2)	1444.086	1	6	4	0	H, CoreF(1305.4)	
				— (B)	1159.5	971.404 (3)	971.404	2	4	5	0	C, CoreF(1305.4), 512(512.3)	
			k-9 (2)	6725 (A, B)	1159.5	1456.605 (2)	1456.602	2	4	5	0	C, (CoreF(1305.4), 512(512.1)) or L ^{by} (658.2), bisectGN(864.3)	
				— (A)	1160.6	1480.098 (2)	1480.097	2	5	3	1	H, CoreF(1305.3), sL ^{ax} (454.3, 512.2, 657.1, 803.2)	
			k-1	6590	1159.3	1006.417 (3)	1006.414	3	5	4	0	C, CoreF(1305.2), L ^{by} (658.3)	
			k-2	6658	1159.4	1011.747 (3)	1011.746	2	6	4	0	H, CoreF(1305.3), L ^{ax} (350.3, 512.1), bisectGN(865.4) [Figure 7, A1]	
				— (A)	1159.3	1517.117 (2)	1517.115	2	6	4	0	H, CoreF(1305.3), 512(512.1)	
				— (A, B)	1160.4	1019.749 (3)	1019.749	1	4	5	1	C, CoreF(1305.4)	
				— (A)	1159.5	1054.760 (3)	1054.760	2	5	4	1	H, CoreF(1305.5), 512(512.2)	
			k-3	6533	1159.5	1074.108 (3)	1074.107	3	5	5	0	C, CoreF(1305.4), L ^{by} (658.1)	
				— (A)	1159.4	1087.442 (3)	1087.443	1	4	6	1	C, CoreF(1305.4)	
				— (A)	1159.5	1122.453 (3)	1122.453	2	5	5	1	C, CoreF(1305.5), 512(512.2)	
			k-5	6782 (A, B)	1159.4	1190.151 (3)	1190.146	2	5	6	1	C, CoreF(1305.3), sL ^{ax} (350.2, 512.2, 657.1, 803.2)	
L	YGN ²⁶⁰ YTCVASNK (1275.555)	5	7, B2	2954 (A, B, C)	1480.6	1078.100 (3)	1078.100	2	4	5	0	C, CoreF(1626.6), bisectGN(1024.9), L ^{ax} (350.3, 512.1) [Figure 7, B1]	
			l-1 (2)	2960 (A)	1479.5	1616.649 (2)	1616.647	2	4	5	0	C, CoreF(1626.6), bisectGN(1024.4), 512(512.2)	
			l-2	2918 (A)	1479.6	1113.114 (3)	1113.111	3	5	4	0	H, CoreF(1625.5), L ^{by} (658.1)	
			l-3	3093	1480.6	1126.446 (3)	1126.446	1	4	5	1	C, CoreF(1626.6)	
				— (A)	1478.0	1161.457 (3)	1161.457	2	5	4	1	H, CoreF(1626.7), sL ^{ax} (350.4, 512.1, 657.2, 803.1)	
			l-4	2905 (A, B)	1479.6	1180.806 (3)	1180.804	3	5	5	0	C, CoreF(1625.6), bisectGN(1024.6), L ^{ax} (350.0, 512.3)	
				3254 (A, C)	1732.4	1059.426 (3)	1059.425	1	3	5	0	C, CoreF(1878.7), bisectGN(1150.6), BA-2	
	HDYGN ²⁶⁰ YTCVASNK (1527.641)	8	—	3176 (A, C)	1731.6	1162.128 (3)	1162.129	2	4	5	0	C, (CoreF(1878.7), L ^{ax} (350.1, 512.2)) or L ^{by} (658.4), bisectGN(1223.8)	

Table 1: Continued

protein	peptides				glycopeptides				N-glycan			
	elution position	Figure	peak no. ^c	scan in Figure 4A ^d	observed peptide-related ion ^e	observed m/z in SIM mode ^b	theoretical m/z ^b	deduced monosaccharide composition				deduced structure ^f (diagnostic ion)
								dHex	Hex	HexNAc	NA	
M	23	7, C2	m-1	LGHTN ²⁷⁹ ASIMLFGPGAVSE (1799,888)	1732.7	1197.144 (3)	1197.139	3	5	4	0	H, CoreF(1877.7), L ^{6y} (512.2, 658.2), bisectGN(1149.1)
				3439	1731.7	1210.475 (3)	1210.475	1	4	5	1	C, CoreF(1877.8), bisectGN(1222.6)
				3383	1732.8	1245.488 (3)	1245.485	2	5	4	1	H, CoreF(1879.7), sL ^{6x} (453.9, 512.2, 657.2, 803.3)
				3080 (C)	1732.7	1264.834 (3)	1264.833	3	5	5	0	C, CoreF(1878.7), bisectGN(1223.4), 512(512.1)
				3553	1731.9	1293.835 (3)	1293.831	1	5	4	2	H, CoreF(1877.6), bisectGN(1150.5)
				3560	1731.9	1294.175 (3)	1294.171	3	5	4	1	C, CoreF(1877.7)
				7299 (C)	1002.6(2)	1101.491 (3)	1101.488	0	3	5	0	C, bisectGN(1286.7) [Figure 7, C1]
				— (C)	1003.1(2)	1141.835 (3)	1141.830	0	5	4	0	H, bisectGN(1286.5)
				7227 (C)	1002.6(2)	1150.176 (3)	1150.174	1	3	5	0	C, CoreF(1075.6), bisectGN(1357.6), BA-2
				7210	1002.7(2)	1190.520 (3)	1190.516	1	5	4	0	H, CoreF(1075.4) or 512(512.0), bisectGN(1359.1)
Kilon	3	8, A2	m-4	7186	1002.8(2)	1244.537 (3)	1244.534	1	6	4	0	H, 512(512.2)
				— (B)	919.5	966.907 (2)	966.907	0	5	2	0	Man-5
				2664 (A, B, C)	919.5	1047.934 (2)	1047.933	0	6	2	0	Man-6 [Figure 8, A1]
				2706 (A, B, C)	919.5	1128.960 (2)	1128.960	0	7	2	0	Man-7
				2679 (A, B, C)	919.4	1209.988 (2)	1209.986	0	8	2	0	Man-8
				5234	972.3	1040.101 (3)	1040.102	0	6	2	0	Man-6
				4760	1765.8	1070.475 (3)	1070.472	1	3	5	0	C, CoreF(1910.8), bisectGN(1167.3), BA-2 [Figure 8, B1]
				4683	1764.7	1105.485 (3)	1105.483	2	4	4	0	CoreF(1910.9), bisectGN(1167.8), 512(512.2)
				4710 (C)	1765.7	1173.176 (3)	1173.176	2	4	5	0	C, CoreF(1911.9), bisectGN(1167.3), 512(512.1)
				4638	1765.8	1275.880 (3)	1275.879	3	5	5	0	C, CoreF(1910.9), 512(512.1)
P	22	8, C2	p-1	— (C)	1098.3(2)	1070.171 (3)	1070.172	0	5	2	0	Man-5
				7203 (C)	1020.3(2)	1401.911 (3)	1401.910	1	5	4	3	C, CoreF(1911.0) Man-5 [Figure 8, C1]
				6895 (C)	1098.3(2)	1070.171 (3)	1070.172	0	5	2	0	Man-5
				6165 (C)	1162.4(2)	1112.871 (3)	1112.870	0	5	2	0	Man-5
				5086 (A, C)	1407.5	1211.037 (2)	1211.036	0	5	2	0	Man-5
				— (B)	1407.7	883.729 (3)	883.730	1	3	4	0	CoreF(1553.5), bisectGN(1061.5)
				LENGOQGIHQ ²³⁸ FFSTR (1834,969)	1098.3(2)	1070.171 (3)	1070.172	0	5	2	0	Man-5
				RLFNGQQGIHQ ²³⁸ FFSTR (1991,070)	1020.3(2)	1401.911 (3)	1401.910	1	5	4	3	C, CoreF(1911.0) Man-5 [Figure 8, C1]
				KRLFNGQQGIHQ ²³⁸ FFSTR (2119,165)	1098.3(2)	1070.171 (3)	1070.172	0	5	2	0	Man-5
				SILVTIN ²⁴⁹ VTQE (1203,635)	1162.4(2)	1112.871 (3)	1112.870	0	5	2	0	Man-5
Q	17	8, D2	q-8 (2)	5086 (A, C)	1407.5	1211.037 (2)	1211.036	0	5	2	0	Man-5
				— (B)	1407.7	883.729 (3)	883.730	1	3	4	0	CoreF(1553.5), bisectGN(1061.5)

Table 1: Continued

protein	sequence ^{a,b}	glycopeptides				N-glycan							
		elution position	Figure	peak no. ^c	scan in Figure 4A ^d	observed peptide-related ion ^e	observed <i>m/z</i> in SIM mode ^b	theoretical <i>m/z</i> ^b	deduced monosaccharide composition				deduced structure ^f (diagnostic ion)
									dHex	Hex	HexNAc	NA	
R HFGN ²⁵⁷ TCVAANK (1380.624)		10	8, E2	q-10 (2)	5059 (A, C)	1407.4	1325.094 (2)	1325.092	1	3	4	0	CoreF(1553.5) or 512(512.2), bisectGN(988.6)
				– (B)	1407.6	951.423 (3)	951.423	1	3	5	0	C, CoreF(1553.6), bisectGN(988.6), BA-2	
				– (A)	1407.6	1426.632 (2)	1426.631	1	3	5	0	C, CoreF(1553.5), bisectGN(988.2), BA-2	
				q-11 (2)	4950 (A, C)	1407.5	1458.635 (2)	1458.634	2	5	3	0	H, CoreF(1553.4), 512(512.2)
				– (B)	1407.3	991.765 (3)	991.765	1	5	4	0	H, CoreF(1553.6)	
				– (A)	1407.6	1487.143 (2)	1487.144	1	5	4	0	H, CoreF(1553.4)	
				q-1	5126 (A)	1407.5	1021.106 (3)	1021.104	1	5	3	1	H, CoreF(1553.4) or 512(512.2)
				– (A)	1407.6	1531.153 (2)	1531.152	1	5	3	1	H, CoreF(1553.6) or 512(512.0)	
				q-2	4885 (C)	1407.4	1026.777 (3)	1026.776	2	6	3	0	H, CoreF(1553.5), L ^{ax} (350.3, 512.2)
				q-2 (2)	4919 (C)	1407.6	1539.663 (2)	1539.660	2	6	3	0	H, CoreF(1554.2), 512(512.1)
				q-3	5010 (A, C)	1407.5	1040.453 (3)	1040.451	2	5	4	0	H, CoreF(1553.6), L ^{ax} (350.2, 512.1)
				– (A)	1407.5	1560.174 (2)	1560.173	2	5	4	0	H, CoreF(1553.4), 512(512.2)	
				q-4	4944 (A, C)	1406.6	1054.128 (3)	1054.127	2	4	5	0	C, CoreF(1552.6)s, L ^{ax} (350.2, 512.1) [Figure 8, D1]
				– (A)	1407.6	1580.687 (2)	1580.687	2	4	5	0	C, CoreF(1553.6), 512(512.2)	
				– (A)	1407.5	1075.121 (3)	1075.122	1	6	3	1	H, CoreF(1554.6)	
				– (A)	1407.6	1612.180 (2)	1612.179	1	6	3	1	H, CoreF(1554.5)	
				q-5	4827	1407.5	1089.139 (3)	1089.137	3	5	4	0	H, CoreF(1553.6), 512(512.1)
				– (A)	1407.5	1094.469 (3)	1094.469	2	6	4	0	H, CoreF(1554.3), L ^{ax} (350.3, 512.2)	
				q-6	5032	1407.3	1102.473 (3)	1102.473	1	4	5	1	C, CoreF(1552.7)
				– (A)	1407.5	1137.486 (3)	1137.483	2	5	4	1	C, CoreF(1553.3), 512(512.2)	
q-7	4869 (A)	1407.6	1156.832 (3)	1156.830	3	5	5	0	C, CoreF(1553.5)				
– (A)	1407.6	1170.166 (3)	1170.166	1	4	6	1	C, CoreF(1553.3) or (sL ^{ax} (512.4, 803.6))					
q-9	5054 (A)	1407.4	1272.870 (3)	1272.869	2	5	6	1	C, CoreF(1553.5) (sL ^{ax} (454.1, 512.2, 657.2, 803.2))				
– (B)	793.2(2)	866.690 (3)	866.690	0	5	2	0	Man-5					
r-7 (2)	3214 (C)	1584.7	1299.536 (2)	1299.531	0	5	2	0	Man-5				
r-1	3339 (C)	1584.6	1010.422 (3)	1010.420	1	3	5	0	C, CoreF(1730.6), bisectGN(1077.0), BA-2				
r-2	3162 (A, C)	1584.7	1050.764 (3)	1050.762	1	5	4	0	H, CoreF(1730.5), bisectGN(1077.7) [Figure 8, E1]				
r-3	3139 (A, C)	1585.9	1085.774 (3)	1085.772	2	6	3	0	H, CoreF(1730.8), L ^{ax} (350.2, 512.2)				

Table 1: Continued

protein	peptides			glycopeptides				N-glycan				
	elution position	Figure	peak no. ^c	scan in Figure 4A ^d	observed peptide-related ion ^e	observed <i>m/z</i> in SIM mode ^b	theoretical <i>m/z</i> ^b	deduced monosaccharide composition				deduced structure ^f (diagnostic ion)
								dHex	Hex	HexNAc	NA	
	r-4			3208 (C)	1585.7	1099.450 (3)	1099.448	2	5	4	0	H, CoreF(1731.7), L ^{a/x} (350.1, 512.1)
	r-5			3189	1584.7	1104.784 (3)	1104.780	1	6	4	0	H, CoreF(1730.6) or L ^{a/x} (350.4, 512.0)
	r-6			3144 (A)	1585.6	1113.127 (3)	1113.123	2	4	5	0	C, CoreF(1730.8), L ^{a/x} (350.1, 512.2)
				— (A)	1585.8	1134.118 (3)	1134.118	1	6	3	1	H, CoreF(1730.6) or 512(512.3)
				— (A)	1584.5	1153.466 (3)	1153.466	2	6	4	0	H, CoreF(1731.6), L ^{a/x} (350.1, 512.2)

^a Theoretical peptide mass indicated in parentheses. ^b Monoisotopic values. ^c Peaks are numbered in decreasing order of their calculated mass. All glycopeptides are triply charged except for doubly charged ions indicated by (2) after the peak number. ^d Glycopeptides were characterized on the basis of alternative LC-MSⁿ runs with conditions indicated in parentheses (A, a C30 column, scan range of *m/z* 1000–2000; B, a C30 column, scan range of *m/z* 700–2000; C, a C18 column, scan range of *m/z* 1000–2000). ^e Y₁ⁿ⁺ or Y_{1a/b}ⁿ⁺, [(peptide + HexNAc + nH)/n]ⁿ⁺; or Y_{1c}ⁿ⁺, [(peptide + HexNAc + dHex + nH)/n]ⁿ⁺. All peptide-related ions are singly charged except for doubly or triply charged ions indicated by (2) or (3). ^f Structures are deduced by MSⁿ: C, complex-type oligosaccharide; H, hybrid-type oligosaccharide; Man-5-9, high mannose-type oligosaccharide containing 5–9 mannose residues; CoreF, trimannosylcore fucose; bisectGN, bisecting GlcNAc; diSia, disialic acid; L^{a/x}, Lewis a/x structure; sf^{a/x}, sialylated Lewis a/x structure; L^{b/y}, Lewis b/y structure; 512, glycan motif consisting of dHex1Hex1HexNAc1. The structure in parentheses indicates the possible structures to be contained in the glycopeptide. ^g Glycosylation was confirmed by Asn-Asp conversion upon PNGase F digestion.

integrated mass spectrum (peaks f-1–9 and g-1–3 in panel F2 of Figure 5) and their MS/MS spectra suggested that complex-type oligosaccharides including Le^{a/x} or Le^{b/y}-modified and/or bisected oligosaccharides and BA-2 are attached to Asn272 (Table 1F).

(vii) *Asn287*. The MS/MS spectra of GPI-linked peptides were selected from all MS data on the basis of the GPI-characteristic oxonium ions, such as GlcN-Ino-PO₄⁺ (*m/z* 422). The structures of the GPI moieties were characterized from their product ions appearing in the MS/MS spectra, and their peptide portions were identified by comparing their observed masses with the theoretical masses of predicted peptides. Figure 4B shows the TIC obtained by GCC-LC-MSⁿ for the hydrophilic glycopeptides. On the basis of the presence of GPI-characteristic oxonium ions, the MS data of GPI-linked peptides were located at position 26. The 9.5% of spectra generated at elution position 26 were assigned to those of GPI-linked peptides of LAMP, OBCAM, and neurotrimin.

Figure 5G shows one of the MS/MS spectra acquired at position 26 (precursor ion, [M + 2H]²⁺ at *m/z* 902.5; peak L2 in Figure 4C). On the basis of the GPI-characteristic oxonium ions, such as NH₂Et-PO₄-Man-GlcN⁺ (*m/z* 447.2), NH₂Et-PO₄-(HexNAc-)Man-GlcN⁺ (*m/z* 650.3), NH₂Et-PO₄-(HexNAc-)Man-GlcN-Ino-PO₄⁺ (*m/z* 910.2), NH₂Et-PO₄-(HexNAc-)(Hex-)Man-GlcN-Ino-PO₄⁺ (*m/z* 1072.2), and GlcN-Ino-PO₄⁺ (*m/z* 422.2), this peptide was identified as the GPI-linked peptide. The product ion at *m/z* 328.3 was assigned to GIN²⁸⁷-NH-Et⁺ on the basis of the fragments that arose by successive cleavages of HexNAc (*m/z* 1600.4), Ino-PO₄ (*m/z* 1340.5), GlcN (*m/z* 1178.3), Man-PO₄-EtNH₂ and Hex (*m/z* 732.2), Hex (*m/z* 570.2), and PO₄-Hex (*m/z* 328.3). In addition, the product ions at *m/z* 732.3 and 1072.2 suggested the existence of HexNAc-(NH₂Et-PO₄)-(Hex)-Man3 in the core structure of GPI (inset of Figure 5G). The presence of a positional isomer was inferred from the acquisition of two different MS/MS spectra of GPI-linked peptides (precursor ion [M + 2H]²⁺, *m/z* 903) at different elution times (Table 2). The alternative runs also suggested the presence of a Hex-Man1 and HexNAc-(Hex-)(NH₂Et-PO₄-)Man3 (peak L1, data not shown, Table 2), and a nonsubstituted Man1 and HexNAc-(NH₂Et-PO₄-)Man3 (data not shown, Table 2) in the GPI core structure.

Glycosylation Analysis of OBCAM. OBCAM has six potential N-glycosylation sites at Asn17, -43, -113, -258, -266, and -279, and the predicted linkage site of GPI is Asn295. From the peptide-related ions, peptides eluted at positions 2, 25, and 7 were estimated to be glycopeptides containing Asn17, -258, and -266, respectively (panels A1–C1 of Figure 6). Panels A2–C2 of Figure 6 show the integrated mass spectrum of glycopeptides obtained from positions 2, 25, and 7, respectively. The glycopeptide containing Asn43 is identical to VAWLN^{38R} in LAMP. From the glycosylation at Asn38 in LAMP, Man-5-9 were inferred to be attached to Asn43 (panel A2 of Figure 5 and Table 1A). Although the MS/MS spectrum of the glycopeptide containing Asn113 (VHLIVQVPPQIMN¹¹³ISSD) was not acquired, glycosylation at Asn113 was corroborated by detection of VHLIVQVPPQIMD¹¹³ISSD after PNGase F treatment (data not shown). The feature of glycosylation at Asn279 was elucidated on the basis of the MS/MS spectra of glycosylated LGNTN²⁷⁹ASITLYGPGAVID which was

protein	peptide (theoretical MW ^b)	peak no. in Figure 4C	scan in Figure 4B	GPI-linked peptide		deduced glycan composition							
				observed peptide-related ion ^b (charge state)	observed <i>m/z</i> ^b (charge state)	Man1			Man3			theoretical MW ^b	
						Hex	Hex	Hex	Hex	HexNAc	P-EtNH ₂		Hex
LAMP	GIN ²⁸⁷ (302.3)	L1	3863	328.3 (1)	983.6 (2)	1	1	1	1	1	1	1	1681.3
		L2	3828 ^c (Figure 5G)	328.3 (1)	902.5 (2)	1	0	1	1	1	1	1	1519.2
			4040 ^c	328.3 (1)	903.1 (2)	1	0	1	1	1	1	1	1519.2
OBCAM	GVN ²⁹⁵ (288.3)	O1	3701 (Figure 6D)	328.2 (1)	821.6 (2)	1	0	0	1	1	1	1	1357.0
		O2	3633 ^d	314.3 (1)	976.5 (2)	1	1	1	1	1	1	1	1681.3
		O3	3853 ^d	314.3 (1)	895.4 (2)	1	0	1	1	1	1	1	1519.2
neurotrimin	VNN ²⁸⁹ (345.4)	N1	3805	314.3 (1)	895.5 (2)	1	0	1	1	1	1	1	1519.2
		N2	3750	314.3 (1)	814.6 (2)	1	0	0	1	1	1	1	1357.0
		N3	3741 ^e	371.2 (1)	1004.8 (2)	1	1	1	1	1	1	1	1681.3
			3896 ^e	371.4 (1)	924.0 (2)	1	0	1	1	1	1	1519.2	
			3873 (Figure 7D)	371.3 (1)	842.8 (2)	1	0	0	1	1	1	1357.0	

^aThe structure of GPI was deduced by another LC-MSⁿ run. ^bAverage value. ^cIsomers. ^dIsomers. ^eIsomers.

acquired in an alternative run with the C30 column (scan range of *m/z* 1000–2000) (Table 1J).

(i) *Asn 17*. As shown in panel A1 of Figure 6, the glycopeptide that eluted at position 2 was assigned to AMDN¹⁷VTVR (and/or AMDN¹²VTVR in neurotrimin) glycosylated with dHex₁Hex₅HexNAc₄NeuAc₄ based on the Y_{1α} ion and the monoisotopic mass of the molecular ion. The attachment of three NeuAc residues in one branch of a biantennary complex type was suggested by the existence of characteristic B ions (*m/z* 495.2, 744.9, and 1239.2) (panel A1 of Figure 6). The molecular ions appearing in the integrated mass spectrum and their MS/MS spectra suggested that most of the glycans at Asn17 were disialic acid-conjugated oligosaccharides (peaks h-1–3 in panel A2 of Figure 6 and Table 1G).

(ii) *Asn258*. Panel B1 of Figure 6 shows the representative MS/MS spectrum of glycosylated ISTLTFN²⁵⁸VSE that eluted at position 25. The monosaccharide composition (dHex₂Hex₅HexNAc₆NeuAc₁) implied two possible structures: a sLe^{ax}-modified core-fucosylated complex type and a Le^{ax} or antigen H-modified core-fucosylated and sialylated complex type (inset of panel B1 of Figure 6). The molecular ions (peaks i-1–2) in the integrated mass spectrum (panel B2 of Figure 6) and the detection of nonglycosylated ISTLTFN²⁵⁸VSE revealed that Asn258 is partly glycosylated with the sLe^{ax} or Le^{by}-modified core-fucosylated complex type, and BA-2 (Table 1H).

(iii) *Asn266*. Panel C1 of Figure 6 shows the product ion spectra of the glycopeptide at position 7, the peptide portion of which was assigned to YGN²⁶⁶YTCVATNK on the basis of the Y_{1α/1β} ion in the MS/MS/MS spectrum. The glycan was characterized as the bisected and core-fucosylated complex-type oligosaccharide containing Le^{ax} structure from the monosaccharide composition (dHex₂Hex₄HexNAc₅), and the Le^{ax}-, bisecting-, and core-fucose-related ions. The MS/MS spectra acquired with other glycoforms (peaks j-1–4 in panel C2 of Figure 6) together with the MS/MS spectra of the glycopeptides DYGN²⁶⁶YTCVATNK (position 13) and KDYGN²⁶⁶YTCVATNK (position 6) suggested that the Le^{ax}-modified and/or bisected complex type and Man-5 were predominantly attached to Asn266 (Table 1I).

(iv) *Asn295*. On the basis of the GPI-characteristic oxonium ions and the peptide-related ion (*m/z* 314.3), the MS/MS spectrum of GPI-linked GVN²⁹⁵ was picked out from position 26 (Figure 6D; precursor ion, *m/z* 976.5; peak O1 in Figure 4C). The fragments arising from the GPI moiety suggested the linkage of Hex to Man1, and HexNAc, Hex, and NH₂Et-PO₄ to Man3 in the core structure (Figure 6D, inset). Furthermore, the MS/MS spectrum of other GPI-linked GVN²⁹⁵ (precursor ion, *m/z* 895; peak O2), which was picked out from position 26 based on the peptide-related ion, suggested that this GPI moiety contained HexNAc-(Hex)-(NH₂Et-PO₄)Man3. Another MS/MS spectrum (precursor ion, *m/z* 814; peak O3) suggested the linkage of GPI moieties containing HexNAc-(NH₂Et-PO₄)Man3 (Table 2). The existence of two isomers was suggested in peak O2 by the acquisition of two MS/MS spectra of GPI-GVN²⁹⁵ (*m/z* 895) at different elution times.

Glycosylation Analysis of Neurotrimin. Neurotrimin contains seven potential N-glycosylation sites at Asn12, -38, -120, -184, -252, -260, and -273, and the predicted linkage site of GPI is Asn289. As the amino acid sequence in the

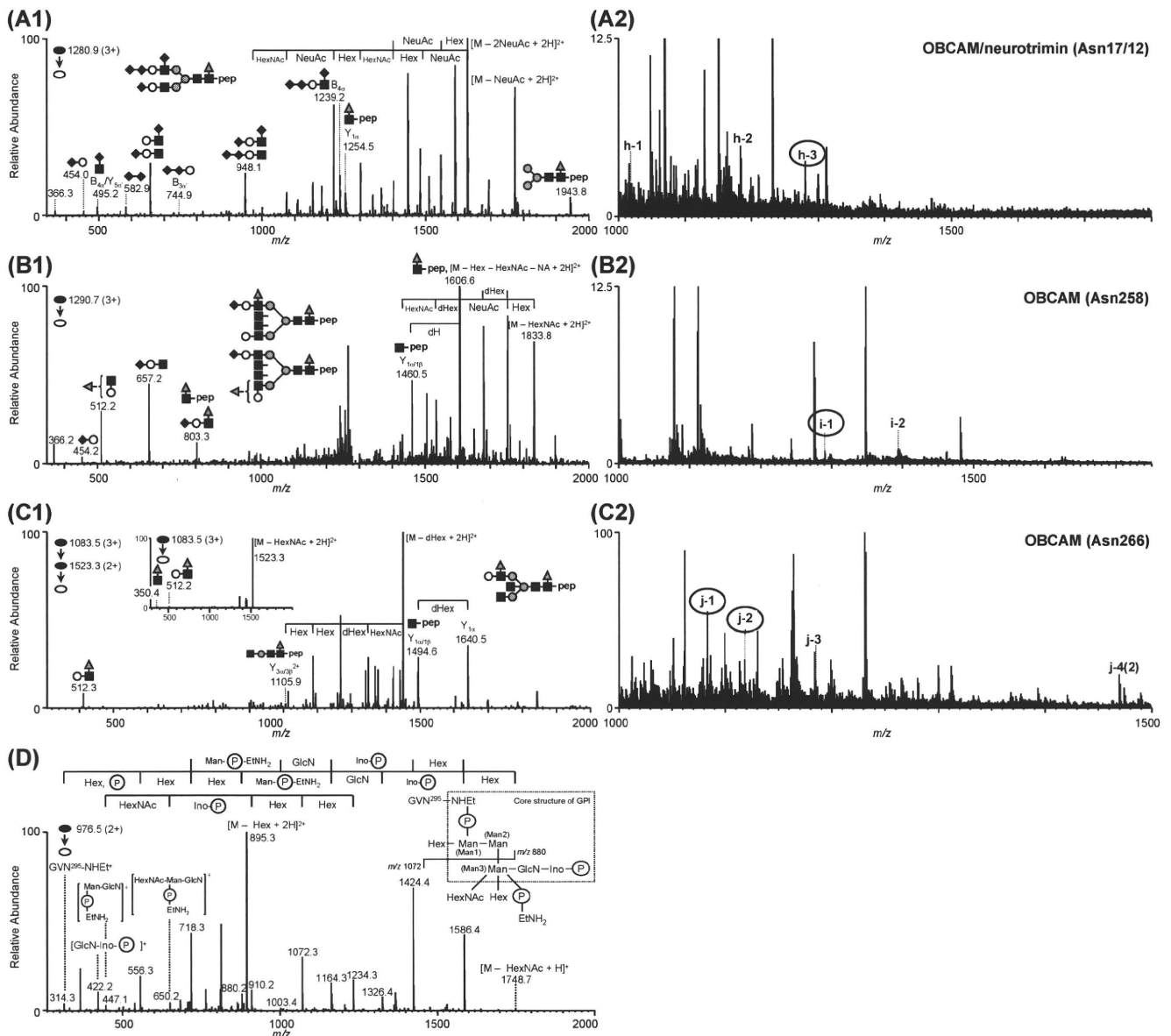


FIGURE 6: MS spectra of OBCAM glycopeptides. (A1) MS/MS spectra of glycopeptide AMDN¹⁷VTVR; elution position, 2; precursor ion, $[M + 3H]^{3+}$ (m/z 1280.9). (A2) Integrated mass spectrum obtained from position 2. (B1) MS/MS spectrum of glycopeptide ISTLTFFN²⁵⁸VSE; elution position, 25; precursor ion, $[M + 3H]^{3+}$ (m/z 1290.7). (B2) Integrated mass spectrum at position 25. (C1) MS/MS and MS/MS/MS spectra of glycopeptide YGN²⁶⁶YTCVATNK; elution position, 7; precursor ion, $[M + 3H]^{3+}$ (m/z 1083.5). (C2) Integrated mass spectrum at position 7. (D) MS/MS spectrum of GPI-linked GVN²⁹⁵; elution position, 26; precursor ion, $[M + 2H]^{2+}$ (m/z 976.5). Symbols are as in Figure 9.

glycopeptide containing Asn12 (GTDN¹²ITVR) in neurotrimin is identical to GTDN¹⁷ITVR in OBCAM, the glycans at Asn12 are estimated to be hybrid and complex types containing disialic acid (panel A2 of Figure 6 and Table 1G). Likewise, the sequence of VAWLN³⁸R in neurotrimin is identical to that of VAWLN³⁸R in LAMP, and therefore, the linkage of Man-5-9 at Asn38 was inferred from the glycosylation at Asn38 in LAMP (panel A2 of Figure 5 and Table 1A). Although the MS/MS spectra of glycopeptides containing Asn120 were not acquired, glycosylation at Asn120 was confirmed by the identification of GND¹²⁰ISLTCIATGR, GND¹²⁰ISLTCIATGRPE, and GND¹²⁰ISLTCIATGRPEPTVTWR after PNGase F digestion (data not shown). The substitution of Asn184 with a Lys or an Arg residue in neurotrimin was suggested as in case of SD rat by the identification of VTVNYPPYISE, which is a fragment of VN¹⁸⁴VTVNYPPYISE (data not shown) (33).

The MS/MS spectra of glycopeptides containing Asn252, -260, -273, and -289 were located at positions 20, 5, 23, and 26 based on the peptide-related ions, respectively (panels A1–C1 and D of Figure 7). The integrated mass spectrum of the glycopeptides containing Asn252, -260, and -273 are shown in panels A2–C2 of Figure 7, respectively.

(i) *Asn252*. Panel A1 of Figure 7 shows the representative MS/MS spectra of glycopeptide LTFN²⁵²VSE linked by dHex₂Hex₆HexNAc₄, acquired at position 20. A Le^{a/x}-modified core-fucosylated and bisected hybrid-type oligosaccharide was deduced from the Le^{a/x}-related ions, and Y_{1β/3α/3β}²⁺ and Y_{1α}. The majority of the glycans at Asn252 are estimated to be Le^{a/x} or Le^{b/y}-modified complex- and hybrid-type oligosaccharides from the molecular ions (peaks k-1–9) in the integrated mass spectrum and their MS/MS spectra (panel A2 of Figure 7 and Table 1K).

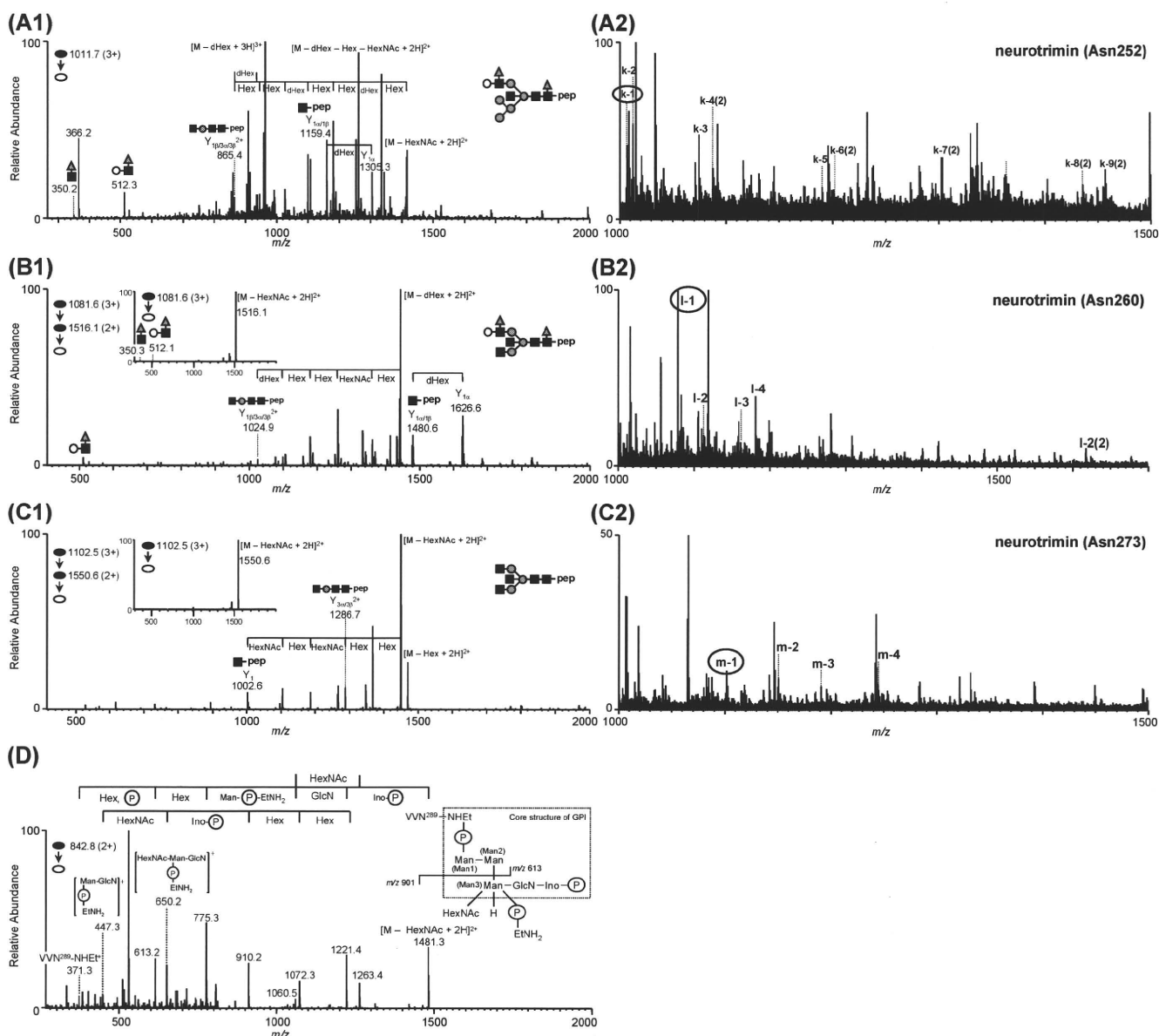


FIGURE 7: MS spectra of neurotrimin glycopeptides. (A1) MS/MS spectra of glycopeptide LTFN²⁵²VSE; elution position, 20; precursor ion, $[M + 3H]^{3+}$ (m/z 1011.7). (A2) Integrated mass spectrum obtained from position 20. (B1) MS/MS and MS/MS/MS spectra of glycopeptide YGN²⁶⁰YTCVASNK; elution position, 5; precursor ion, $[M + 3H]^{3+}$ (m/z 1081.6). (B2) Integrated mass spectrum at position 5. (C1) MS/MS and MS/MS/MS spectra of glycopeptide LGHTN²⁷³ASIMLFPGAVSE; elution position, 23; precursor ion, $[M + 3H]^{3+}$ (m/z 1102.5). (C2) Integrated mass spectrum at position 23. (D) MS/MS spectrum of GPI-linked VNN²⁸⁹; elution position, 26; precursor ion, $[M + 2H]^{2+}$ (m/z 842.8). Symbols are as in Figure 9.

(ii) *Asn260*. Panel B1 of Figure 7 shows the representative product ion spectra of the glycopeptide eluted at position 5, the peptide portion of which was identified as YGN²⁶⁰YTCVASNK on the basis of the $Y_{1\alpha/1\beta}$ ion in the MS/MS/MS spectrum. The monosaccharide composition (dHex₂Hex₄HexNac₅), the Le^{alx}-related ions in the MS/MS spectrum, and the presence of $Y_{1\beta/3\alpha/3\beta}^{2+}$ and $Y_{1\alpha}$ in the MS/MS/MS spectrum revealed the linkage of a Le^{alx}-modified fucosylated and bisected complex-type oligosaccharide to this peptide (inset of panel B1 of Figure 7). The molecular ions in the integrated mass spectrum (peaks l-1–4 in panel B2 of Figure 7) together with the MS/MS spectra of glycosylated HDYGN²⁶⁰YTCVASNK (position 8) suggested that Asn260 was predominantly glycosylated with the Le^{alx} or Le^{bly}-modified bisected complex- and hybrid-type oligosaccharides and BA-2 (Table 1L).

(iii) *Asn273*. On the basis of the Y_1 ion and the monoisotopic mass, the glycopeptide eluted at position 23 was assigned to LGHTN²⁷³ASIMLFPGAVSE glycosylated with Hex₃HexNac₅ (panel C1 of Figure 7). Its glycan moiety was characterized as a bisected agalacto-complex-type oligosaccharide based on $Y_{3\alpha/3\beta}^{2+}$. Other glycans at Asn273 were assigned to bisected complex- and hybrid-type oligosaccharides (peaks m-1–4 in panel C2 of Figure 7 and Table 1M).

(iv) *Asn289*. Figure 7D shows one of the MS/MS spectra of GPI-linked VNN²⁸⁹, which was picked out from position 26 on the basis of the peptide-related ion (peptide-NH-Et⁺, m/z 371.3). Three different MS/MS spectra of GPI-linked VNN²⁸⁹ were picked out from position 26 (Figure 4B). From the molecular ions [peaks N1 (m/z 1004), N2 (m/z 924), and N3 (m/z 842)] and their fragments, it was suggested that they contain Hex-Man1 and HexNac-(Hex-)(NH₂Et-PO₄)Man₃,